INTERACTION BETWEEN SHOCK WAVES AND TURBULENT OR TRANSITIONAL BOUNDARY LAYERS AT MACH NUMBER 3

A Thesis Submitted To The
Faculty of the Graduate School of the
University of Minnesota

by

Edelbert E. Irish
Lt. U.S.Navy

In Partial Fullfillment of the Requirements
for the Degree of
Master of Science in Aeronautical Engineering

May 1957

ACKNOWLEDGEMENTS

The author wishes to express his appreciation to Dr. Rudolf Hermann of the Aeronautical Engineering Department of the University of Minnesota for his interest and advice; to Mr. Fred Moynihan of the Rosemount Aeronautical Research Laboratory of the University of Minnesota for his assistance and advice; to Mr. Miles Mock and Mr. Mike Schonberg mechanics in the Aeronautical Engineering Department for their valuable suggestions and most skilful fabrication of the equipment; to the U.S. Naval Postgraduate School for sponsoring the author's attendance at the University of Minnesota; and last, but not least, to his wife for her encouragement and understanding throughout the author's period of post graduate study.

TABLE OF CONTENTS

	page
SUMMARY	
INTRODUCTION	1
SYMBOLS AND NOTATIONS	4
EQUIPMENT	5
EXPERIMENTAL PROCEDURE	9
RESULTS	11
DISCUSSION	16 - 31
Preliminary Analysis	16
Shock Wave Types	19
Boundary Layers Turbulent Over Interaction Region	22
Boundary Layers Laminar Initially But Turbulent In The Transition Range	27
CONCLUSIONS	32
REFERENCES	34
APPENDIX 1	37

SUMMARY

An experimental study has been made of the interaction phenomena between the boundary layer on a smooth flat plate and an externally generated shock wave at a Mach number of about 3.0. Flat plate static pressures and shadowgraphs were used to make the study. A range of boundary layer Reynolds numbers (1.01×10^6 - 2.40×10^6), extending from the transition region to the low turbulent range, and shocks of varying strength and of the impulse and step wave types have been covered.

Variations in these parameters were found to determine the type of interaction and to affect the upstream influence of these interactions. The pressure ratios at separation were found to be independent of the shock strength but to be dependent on the state of the boundary layers, i.e. pressure ratios required to separate turbulent boundary layers were about double those required to separate laminar. The size of the separated region was found to be an important characteristic because the pressure gradients appear to be larger when the separated region is small.

INTRODUCTION

The existence of fluid viscosity and the subsequent adherence of the fluid to the body results in a boundary layer build up over the body. These viscous effects produce large deviations in actual supersonic flows from those predicted by potential theory and particularly adverse pressure gradients have been found to greatly affect these changes. Theoretical prediction of these viscous effects is not well defined for turbulent boundary layers at either low or high speeds. It is known that these large deviations are of considerable importance in such supersonic flow regions as flow through engine intakes, flow past wings, and flow through supersonic wind tunnel diffusers. In such cases shock waves strike the boundary layers on these surfaces and interact to give a flow pattern which has little resemblance to that expected in the absence of viscous effects.

This paper is then concerned with the interaction between shock waves of varying strength, and the boundary layer on a smooth flat plate which is either turbulent or in the transition region with separated and unseparated flow. In all cases the shock waves

were generated by wedges fully spanning the tunnel as did the flat plate. The study was made by means of a static pressure survey along the plate and optically by use of shadowgraphs.

The shock wave-boundary layer interaction problem was first noted by Ferri in 1939, Ref. 1. During the past few years, the shock wave interaction problem has been the subject of much theoretical and experimental study. The work of Liepman, Ref. 2, and others, Refs. 3 and 4, have provided much experimental data on the interaction of shock waves with laminar boundary layers. Considerable progress has been made with theoretical studies of both laminar and turbulent boundary layer-shock wave interactions, Refs. 5, 6, and 7. Experimental data on the interactions of shock waves with turbulent boundary layers has been provided by Refs. 4, 8 and 9. However, much more data and study is required to provide a better insight into the interaction phenomena.

This paper then presents some experimental results applicable to this yet somewhat unsolved problem of predicting the viscous effects in turbulent boundary layers with adverse pressure

gradients. Particular note is made that these results are for Reynolds numbers in or just above the region where transition to turbulent flow occurs.

This work was carried out in the 1-3/4 x 2-inch blow-down supersonic wind tunnel at the Rosemount Aeronautical Research Laboratory of the University of Minnesota. The author was assisted by Lt. W.W. Koepcke U.S.N., who conducted a study of an associated problem.

SYMBOLS AND NOTATIONS

d	upstream effect of the shock wave
p	static pressure
p_∞	free stream static pressure
p_K	static pressure at the "kink" in the pressure profile for turbulent boundary layers
p_T	static pressure at the top of the laminar step on pressure profile
q_∞	free stream dynamic pressure, $\frac{\gamma p_\infty}{2} M_\infty^2$
s	length of laminar step on pressure profile
x	distance along flat plate measured from the leading edge
x_t	distance along a fictitious wholly turbulent flat plate see p. (14)
C_p	pressure coefficient, $\frac{p - p_\infty}{q_\infty}$
M_∞	free stream Mach number
Re_x	Reynolds number at station x
Re_{x_t}	Turbulent Reynolds number
θ	nominal wedge angle (flow defelction, degree)
δ	boundary layer thickness
δ^*	boundary layer displacement thickness

EQUIPMENT

A complete account of the equipment design used in this investigation is given in Appendix 1.

Flat Plate - The flat plate used in this investigation, Fig. 1 (a), was 1.75 inches wide by 4.50 inches long and 0.125 inches thick. The leading edge was made as sharp as possible by a 5 degree wedge angle on the underneath side. After the working surface was made as smooth as possible by hand working, it was then finished by a commercial chrome plate over the entire surface. Five static pressure taps 0.006 inches in diameter were placed as shown in Fig. 2. The longitudinal spacing of these holes was 0.25 inches on centers with the first hole 0.725 inches aft of the leading edge. This spacing was chosen to obtain a Reynolds number variation. The static pressure leads were 0.3125 inches in diameter and were lead back into the diffuser section and then out through a pipe plug in the diffuser side wall. The leading edge thickness of the flat plate varied from 0.0015 inches on the left side to 0.0005 inches on the right side.

Shock Generators - The shock generators shown in Fig. 1 (b), ware half wedges which were movable relative to the fixed flat plate. In this manner the position of the shock wave-boundary layer intersection point could be varied relative to each pressure tap. Since one of the parameters to be investigated was the interaction effects due to shock strength, wedge angles of 5, 10 and 15 degrees were used. The limit of 15 degrees is explained in Appendix 1. For turbulent flow these three wedge angles do give the effect for weak, medium and strong shocks, respectively.

The leading edge thickness of the wedges was:

(1). for the 1/8 inch, 5 degree wedge .0003 inches.

(2). for the 1/8 inch, 10 degree wedge .0011 inches.

(3). for the 1/4 inch, 15 degree wedge .0006 inches.

Wind Tunnel - The wind tunnel shown in Fig. 3, had a test section 1.75 inches wide and 1.94 inches high. Glass side windows permitted observation of both the flat plate and the wedge and photographing the flow. The tunnel was operated by blow-down from a high pressure air supply to atmosphere and to vacuum tanks. The tunnel had a fixed nominal Mach Number 3 asymmetric nozzle of which the plastic contoured side was compensated for boundary layer growth. The steel flat

sided nozzle block was not compensated for boundary layer growth. A static pressure tap in this block was located just ahead of the flat plate leading edge position.

Lead Screw Mechanism - A novel means of accurately positioning the wedges was provided by means of the lead screw mechanism. The wedge pylon was placed in a "T" slot recessed in the upper plastic nozzle block. A lead screw operating through a brass plug in the flange between the tunnel test section and the diffuser section was attached to the wedge pylon in such a manner that the pylon could be moved fore and aft in the slot by turning the lead screw, see Fig. 4. The lead screw pitch was 40 threads per inch or one turn was equivalent to .025 inches.

Pressure Measuring Apparatus

Manometers - The static pressure survey along the flat plate was measured on a multi-tube manometer using mercury and the reservoir of which was vented to the atmosphere. The manometric scale was calibrated in inches of mercury. The manometer board was equipped with valves such that the tubes

could be closed off after each run and the data could then be recorded. The pressure in the stagnation chamber was measured on a U-tube manometer calibrated to read centimeters of mercury, gage.

Stagnation Chamber Temperature - The stagnation chamber temperature was measured by means of a shielded thermocouple in the stagnation chamber. The temperature was read from a Leeds and Northrup potentiometer indicator.

Shadowgraph Equipment - A shadowgraph method for viewing and photographing the shock waves in the test section was employed. A mercury arc light source using a Kh-6B power supply was used for illiminating the test section. A switch permitted operation of the light source either as a constant source for viewing or as a flash for photographing the flow conditions in the test section. The duration of the flash was approximately three microseconds.

EXPERIMENTAL PROCEDURE

The previously described equipment was set up and used in the following manner. The 5° wedge was placed in its most aft position such that the interaction region did not influence the pressure on any of the pressure taps. In this position a run was made to obtain the Mach distribution curve over the flat plate shown in Fig. 5. Based on theoretical calculations the wedge was then positioned such that the shock was on pressure tap 5, the tap furthest aft. The wedge was then moved aft in equal increments until tap 5 was out of the interaction zone, i.e. the static pressure was constant. The wedge was then placed again with the shock on tap 5 and moved forward in equal increments until tap 1 passed out of the interaction zone, in this case when the peak pressure was passed.

The tunnel was not operated continuously, but was started each time for each wedge position. Each run had a duration of between 30 and 45 seconds. Since the 15 degree wedge was operated so closely to the choked condition (see Appendix 1), it was sometimes necessary to surge the stagnation pressure to drive the normal shock downstream before reducing

the stagnation chamber pressure to running conditions. In each case when the stagnation pressure was constant and the tap pressures, on the multi-tube manometer, had stabilized the manometer board was closed off and the tunnel was shut down. The wedge position, stagnation temperature and manometer readings were recorded after each run.

After an initial rough plot of this data was made, re-runs to fill in the curves near inflection points and to substantiate doubtful points were then made. By keeping track of the stagnation temperatures and matching Reynolds number and stagnation pressure accordingly, good results were obtained on nearly all of the re-run data. All of the desired data, except photographs, were taken for each wedge before it was removed and another put in its place. The data was taken using the wedges in the following order:

(1). the 10 degree wedge.

(2). the 5 degree wedge.

(3). the 15 degree wedge.

RESULTS OF THE EXPERIMENTAL STUDY

Static pressure distributions are given for shock wave-boundary layer interaction as functions of shock strength, Reynolds number and shock wave type for boundary layers turbulent over the entire interaction region and for boundary layers in the transition region such that they are laminar at separation but change to turbulent before reattachment. The results for the turbulent interactions for three shock strengths and for three Reynolds numbers are presented in Figs. 6, 7, and 8. A summary of the pressure distributions for three shock strengths for a typically turbulent interaction is given in Fig. 9. Similarly the results for the transitional interaction for two shock strengths and for two Reynolds numbers are presented in Figs. 10 and 11. A pictorial presentation of the shock wave boundary layer interaction details is given in Fig. 12.

The zero coordinate position is the theoretical intersection of the shock wave with the flat plate, as calculated by the wave angle and a known fixed reference for the wedge shock generator. A check on these theoretical positions was made using shadowgraphs. The negative points on the abscissa

indicate distances of the pressure tap upstream and the positive points indicate distances of the pressure tap downstream of the theoretical shock impingement position. The vertical coordinate is the static pressure ratio p/p_∞ where p_∞ is the static pressure of the undisturbed flow measured at the lower tunnel wall just ahead of the flat plate leading edge. The free stream static pressure was considered to be the most stable reference since it was recorded for each data run whereas the stagnation pressure was not recorded nor could it have been recorded as accurately. Since the Mach distribution over the flat plate varied as shown in Fig. 5, the value of p/p_∞ differed from unity for each profile. This variation from unity was reflected by the Mach distribution curve for which a zero pressure gradient was assumed. Therefore, each profile was shifted accordingly to give a uniform reference, the pseudo $p/p_\infty = 1$. The Reynolds number per inch was fixed through out this study since any small stagnation temperature variation was corrected by the appropriate change in the stagnation pressure. Hence the Reynolds number variation in this study was obtained by the variation in the tap locations.

The Reynolds number at the point of pressure measurement is noted for each pressure profile.

One sees that for each pressure profile that the tap Reynolds number is constant, but the Reynolds number of the incident shock position is variable. For each shadowgraph picture, however, the tap Reynolds number would be a variable and the incident shock position Reynolds number would be constant. Therefore, a complete correlation between the pressure profiles and the corresponding shadowgraph pictures can not be made. From Figs. 6, 7, and 10 the actual interaction lengths for these profiles are seen to be relatively short and the above mentioned variations, therefore, should be nearly negligible. The interaction lengths for the profiles given in Figs. 8, and 11 are observed to be about three times the lengths of those given in Figs. 6, 7, and 10. Thus an appreciable variation in the incident shock position Reynolds number occurs for each pressure profile and correspondingly an appreciable variation in the tap Reynolds number occurs for each shadowgraph.

The state of the boundary layer, laminar or turbulent, was not determined experimentally, but

is generally based on the value of the Reynolds number relative to that expected for transition, from Ref. 10. Also, from previous work done in this tunnel, Ref. 11, the lower transitional Reynolds number limit was rather well defined at approximately 800,000. However, no upper limit for completion of transition was established. The pressure rise required to cause boundary layer separation was indicative of the boundary layer conditions at the beginning of the interaction. For each shock strength the theoretical pressure jump for incident shock wave plus the associated reflection is noted on the pertinent figures and was determined by use of the computational curves of Ref. 12. Slight differences in the flow conditions in the tunnel can lead to slightly different effective wedge angles. The shock wave angles used in determining the theoretical pressure jump was measured directly from the shadowgraphs.

The turbulent Reynolds number, Re_{x_t}, was determined in the following manner. The operating Reynolds number per inch defined by the operating stagnation temperature and pressure was multiplied by a characteristic length x_t, where x_t is defined

as the distance from the leading edge of a fictitious wholly turbulent flat plate to the test point. The position of the fictitious leading edge was estimated from the calculated position of transition to turbulent flow, assuming momentum thickness to be continuous at transition. This will be discussed at greater length in the next section.

The value of the boundary layer displacement thickness, δ^* was calculated from the relation given in Ref. 7, and is

$$\delta^* = \frac{0.0475\,(1 + 0.35 M_\infty^2)}{\left(1 + 0.88\,\frac{\gamma-1}{2}\,M_\infty^2\right)^{0.44}} \frac{x_t}{(Re_{x_t})^{1/5}}$$

The boundary layer thickness, δ , was determined from the empirical relation $\delta^*/\delta = 0.33$ at Mach 3, also given in Ref. 7.

DISCUSSION OF EXPERIMENTAL RESULTS

Preliminary Analysis - In order to make any kind of a quantitative analysis of the shock wave-boundary layer interaction it is necessary to first determine what parameters are meaningful in such a study. Early theoretical studies Refs. 13 and 14 attempted to explain the interaction effects in terms of the disturbance propagated upstream through the region of subsonic flow in the boundary layer. Experimental results, however, showed that the upstream influence predicted by such a theory was smaller than the effects actually obtained.

More recently theories have been advanced by Refs. 5, 7, 15, and 16, dealing with boundary layer separation ahead of the incident shock. Some of the parameters considered in these theories are the upstream influence of the interaction, the shock strength, the Mach number, and the boundary layer Reynolds number. In this study the shock strength, designated by the shock deflection angle θ , was varied by the use of half wedges with different deflection angles. The boundary layer

Reynolds number was varied by varying the tap location. The Mach number in this study was constant. The upstream influence, the distance d, was analyzed in terms of the boundary layer displacement thickness δ^*, calculated from the above formula assuming no presence of a shock.

The data analysis is thus obvisouly dependent to a large extent on the proper determination of the turbulent Reynolds number, Re_{x_t} . In order that Re_{x_t} may be determined accurately, it is first necessary to accurately locate the effective leading edge of the turbulent boundary layer or the leading edge of the fictitious wholly turbulent flat plate described previously. Realizing that as the shock strength increases the adverse pressure gradient increases and causes transition to take place earlier and also realizing that transition at each shock strength would be a function of the position of the shock along the flat plate, a systematic study was made of the variation of d/δ^* as a function of the turbulent Reynolds number, Re_{x_t} .

From previous work in this tunnel, Ref. 11 the lower transitional Reynolds number was found to be about 0.8×10^6 . The position of transition, the distance downstream of the leading edge of the

flat plate, based on this Reynolds number was determined to be 0.575 inches. The leading edge of the fictitious turbulent flat plate was then assumed to be half way between the leading edge of the flat plate and the transition point, or 0.288 inches. This then makes the maximum possible error 50% and the probable error about 25%, if transition occurs at a Reynolds number of 0.8×10^6 . After looking at the pressure profiles for the various tap locations along the flat plate, it appeared that the forward holes would probably induce early transition. Therefore, two other positions were assumed for the position of the leading edge of the fictitious flat plate, one 25% and one 75% of the previously determined distance to the transition point. Therefore, the fictitious flat plate leading edge positions used here were 0.144, 0.288 and 0.432 inches aft of the flat plate leading edge. A plot of d/δ^* vs Re_{x_t} , where x_t was determined for each tap for each of the three above reference points, is shown in Fig. 13. From this presentation it can be seen that the position of the reference point makes no

appreciable difference on variation of d/δ^* with Re_{x_t} . Therefore, the remainder of the analysis will be based on the mean reference position previously assumed, namely the reference position 0.288 inches aft of the flat plate leading edge.

Shock Wave Types - Shock waves will first be discussed here in a general manner in order to understand how they affect the results obtained in this study. A more rigorous discussion is given by Liepman in Ref. 2. The two types of shock waves considered here are the "impulse-type" and the "step type".

The impulse type wave is one in which a sharp compression wave is immediately followed by an expansion. In the two dimensional case here, the expansion resulted when the flow has been deflected by the nose of the wedge and was then expanded aroundthe corner at the back of the wedge until the flow was parallel to its original direction. The pressure distribution in such a case would be such as to increase to some peak value (depending on the proximity of the expansion to the compression wave) and then drop off to approximately the value of the original pressure. A typical impulse type wave is shown in Fig. 14 (a).

For the step wave first consider a normal shock in an ideal fluid. The pressure distribution under such conditions would be an instantaneous "step" from one static pressure to a higher pressure. Similarly, the pressure distribution through an oblique wave, as from the vertex of a wedge, is also a step wave. A typical step wave is shown in Fig. 14 (b).

A. Comparison of Reflections of Shock Wave Types.

A study of the differences in the reflections of impulse and step shock waves made by Liepman showed the following general characteristics. For the impulse type wave the laminar boundary layer resulted in a smoothing of the pressure profile. That is the peak pressure was much lower than the theoretical pressure rise across the compressive shock wave alone. The turbulent boundary layer, though not as pronounced as the laminar did produce a peak pressure which was still below the theoretical pressure. In the case of the step wave the laminar boundary layer actually resulted in a peak pressure slightly greater than the theoretical value. And again the pressure rise through the turbulent boundary layer was not quite up to the theoretical value. It was noted that the upstream effects for impulse type

waves looked much like those for step waves.

B. Shock Wave Types Applied To The Experimental Data.

The results of this investigation arise from a combination of these two shock wave types. As shown in Fig. 15, the 5 degree wedge should give typically step wave results and the 10 and 15 degree wedges should give results like impulse-type waves because of the relatively small distance at the flat plate surface between the incident compression waves and the expansion fan from the back of the wedge. These distances are 0.916, 0.152, and 0.259 inches for the 5, 10 and 15 degree wedges respectively. For the shock strengths $\theta=10^{\circ}$ and $\theta=15^{\circ}$ a vertical line at the top of each pressure curve indicates the position at which the expansion fan from the back of the wedge strikes the boundary layer.

Comparing the profiles of Figs. 6 and 10, one sees the general step wave results anticipated. That is the initially laminar profiles have higher pressure rises than do the turbulent profiles with the exception of curve for tap number three of Fig. 6. Though curve for tap number three at shock strengths of $\theta=5^{\circ}$ and $\theta=10^{\circ}$ is not typically laminar it does appear to have a somewhat laminar profile at the

shock strength of $\theta=15^{\circ}$ which may account for its high peak value at $\theta=5^{\circ}$.

Curve for tap number five for $\theta=10^{\circ}$, Fig. 7, exhibits a typical impulse type curve because the pressure drops off after the peak to nearly the value of p_{∞} . The pressure profiles for $\theta=10^{\circ}$, Fig. 7 and 11, do not agree wholly with the results of Ref. 2, in that the laminar profiles do not peak at a lower pressure than the turbulent profiles. However, the distance between the expansion fan and the shock wave is different from that given in Ref. 2, and the boundary layers in the case of the laminar profiles is in the transition region.

The pressure profiles for the $\theta=15^{\circ}$, Fig. 8, also indicate an impulse-type shock wave though the data for these profiles are not complete.

Boundary Layers Turbulent Over Interaction Region

A. Flow Pattern and Pressure Profiles At The Flat Plate.

For weak shocks the shock strength was not strong enough to cause separation. Such was found to be the case for the 5 degree flow deflection and as seen in Fig. 6, a nearly inviscid type reflection occurs. The pressure rise at the surface begins

about 3.5 boundary layer thicknesses ahead of the shock.

Moderate shock strengths result in a slight departure from the regular (nearly inviscid) reflection and the overall interaction region spreads out slightly as shown in Fig. 7 for $\theta=10^{\circ}$. Here the pressure rise began about 5.5 boundary layer thicknesses ahead of the shock. Ref. 9, foundthat for shock strengths above $\theta=9^{\circ}$ separation occured at a static pressure ratio of approximately 2.0 - 2.1. Fig. 7, indicates a small separation occurs at a static pressure ratio of about 2.1 and a triply inflected profile results. The pressure gradient remained nearly constant between the separation point and the reattachment point. This effect was noted in Ref. 17, and was attributed to the fact that the separated region does not thicken enough between transition and the shock for the pressure gradient to be appreciably affected. The association between thickness of the separated region and the pressure gradient along with an explanation of the inflection points is given in detail in the section on Boundary Layers Laminar Initially.

For very strong shocks the separation becomes more pronounced and static pressure distribution is as shown in Fig. 8 for $\theta=15^{\circ}$. The interaction length increases considerably to approximately 25 boundary layer thicknesses. Though this interaction length could be 20 - 30 per cent in error because of an error in Re_{x_t} , this value would still be large compared with the nominal value of 10 interaction lengths given in Refs. 9, 17 and 18. This would indicate that the Reynolds numbers here are still somewhat in the transitional region. Separation still occurs at a static pressure ratio of roughly 2.1. The pressure rises sharply to the separation point after which the pressure gradient decreases until approximately the point at which the incident shock wave strikes the boundary layer. Downstream of this point the pressure gradient rises until roughly the reattachment point is reached where it then begins to decrease.

When an appreciable amount of separation does occur, the boundary layer just upstream of the separation thickens and thus deflects the free stream flow. A band of compression waves is thus generated which is visible in Fig. 12 (c) 4.

B. Upstream Influence.

The upsstream distance, d, which the interaction affected, was studied in terms of the boundary layer displacement thickness δ^*, of the undisturbed flow just ahead of the interaction zone. It was determined that d/δ^* was unaffected by Reynolds number for the weak shock, $\theta = 5^\circ$. However, d/δ^* was found to decrease with increasing Re_{x_t}, turbulent Reynolds number, approximately as $(Re_{x_t})^{-4/3}$ for $\theta = 10^\circ$ and 15°. Ref. 17, found very little if any systematic variation in d/δ^* with Reynolds number. The variation with Re_{x_t} found in the results of this study tend to bear out an earlier observation, namely, that over the range of Reynolds numbers tested here the boundary layer is in the transition region throughout. The magnitude of the upstream effect with changes in shock strength is shown in Fig. 16, the measured values here are plotted against p_{max}/p_∞ superimposed on the results found in Ref. 4. Again we see as the turbulent Reynolds number becomes larger, that is more truly turbulent, the values more nearly agree with those of Ref. 4.

Further evidence of the transitional effects in these results is seen when a comparison is made

with the results of Ref. 18. In Ref. 18, a semi-emperical relation was derived between the apparent shock thickness for normal shocks at Mach number 1.5 and Reynolds number. Here the apparent shock thickness, measured between the maximum and the minimum tap pressure and made dimensionless by dividing by x_t , is plotted against the turbulent Reynolds number at the tap as shown in Fig. 17. The differences between the turbulent and the transitional values of the parameters compared here are magnified as the shock strength increases.

C. Conditions In The Vicinity Of Separation

When separation occurs, one observes the bend in the pressure profiles in the vicinity of the boundary layer separation point. Ref. 19, locates the pressure at this "kink" by the intersection of the maximum and minimum slopes tangent to the profile, e.g. see Fig. 7. The pressure coefficients at these defined points, $C_{p_K} = \frac{p_K - p_\infty}{q_\infty}$, were found to increase slightly with turbulent Reynolds number Re_{x_t} , as shown in Fig. 18. Ref. 19, found a very slight tendency for these pressure coefficients to decrease, but the tendency was so small the variation was considered negligible. The pressure ratio at

separation appeared to be independent of the shock strength, which was noted previously by Ref. 7.

Bouhdary Layers Laminar Initially But In The Transition Region

A. Flow Pattern and Pressure Profiles At The Flat Plate.

Since the Reynolds number of the boundary layer just ahead of the interaction region is in the transition range, transition should occur shortly after separation in each case. The pressure profiles of this study show that the point of transition relative to the theoretical shock position varies with the shock strength. As the shock strength increases the position of transition moves upstream from the shock position. When the shock strength is strong $\theta=10^{\circ}$, as in Fig. 11, the pressure distribution may have five inflection points as compared to three for turbulent boundary layers with strong shocks, also. These are:

(1). Where the boundary layer is initially laminar a step occurs as the boundary layer separates because the pressure gradient falls off after separation. (The reason for this is discussed below)

(2). When transition occurs the boundary layer becomes capable of withstanding a larger adverse pressure gradient and thus the pressure profile rises.

(3). As the separated region becomes thicker the turbulent shear and friction forces acting on it can not support a large adverse pressure gradient and the pressure gradient drops off again.

(4). When the shock strikes the boundary layer, the flow is deflected towards the plate and the separated region becomes thinner and the pressure profile again rises.

(5). When the boundary layer reattaches, downstream of the reattachment point the pressure gradient falls again.

The general features of such a profile are observable in the flow conditions shown in Fig. 12 (b) 1. The drops in pressure gradient, at inflection points 1 and 3 above, can be explained in the following manner. Following the interaction model developed by Holder, Ref. 17, and described above, then downstream

of the separation point a dead air region* forms near the wall and grows thicker as it proceeds on downstream. When the dead air region grows thicker, the boundary layer cannot support as large an adverse pressure gradient as before and thus the reason for the laminar step. This result becomes apparent when one considers the shear stress distribution through the boundary layer and the resulting shear forces acting on the dead air region balancing the forces due to the adverse pressure on the same region.

When the shock strength is not so strong $\theta = 5^{\circ}$, as in Fig. 10, the pressure profile has only three inflection points like the separated turbulent case. Here between transition and the reattachment point a generally steady pressure rise takes place.

B. Upstream Influence

The upstream distance, d, is seen to decrease as the Reynolds number increases and at the same time the length of the laminar step also decreases.

* The dead air region or separation region was a region of effectively no flow, i.e. the Mach number varied from some small positive value to a negative value (reversed flow).

This occurs because the separation point moves closer to the transition point which is nearly fixed relative to the shock position on the flat plate, as shown in Fig. 10 and 11. The upstream distance in terms of undisturbed displacement thickness decreases with increasing Reynolds number approximately as $(Re_x)^{-4/3}$. No correlation with the results of others is possible in this particular regime. However, these results are shown in Fig. 19, superimposed on the results found in Ref. 17, for which the boundary layers were laminar at separation but turbulent before reattachment and for which the Reynolds numbers of the boundary layer just upstream of the interaction region were appreciably less than the Reynolds number of transition to turbulent flow.

C. Separation and Transition

The pressure profiles characterized by the laminar step where separation occurs somewhere on the steep part of the curve presumably at or near the first inflection point. Separation was thus found to occur at a static pressure ratio of

about 1.10 ± .01 compared to 2.07 ± .12 for a turbulent boundary layer. The pressure ratio at separation of 1.10 ± .01 for the boundary layers in the transitional region compared to the separation pressure ratio of 1.12 ± .05 for completely laminar boundary layers, Ref. 20, shows that there is no variation in the separation pressure ratio and that it is a function only of the state of the boundary layer at the beginning of the interaction. The laminar step was broken where transition began. The length, s , of this laminar step decreased with increasing Reynolds number approximately as $(Re_x)^{-2}$ is shown in Fig. 20. The pressure coefficient, $C_{p_T} = \frac{p_T - p_\infty}{q_\infty}$, at roughly the top of this laminar step varied as $(Re_x)^{-1/5}$ shown in Fig. 21.

CONCLUSIONS

From the results of this investigation of the interaction between externally generated shock waves and boundary layers turbulent or in the transitional region, the following conclusions were made.

1. Two distinct types of interaction are shown. In one the boundary layer is laminar initially but it separates and transition to turbulent flow occurs. In the other turbulent flow exists through out either separated or unseparated.

2. Factors determining the above are the boundary layer Reynolds number and shock strength.

3. Upstream effects for turbulent boundary layers that are not fully developed appear to be greater than those expected for completely turbulent conditions. These upstream effects appear to be independent of Reynolds number if fully turbulent flow exists though at the higher shock strength it was found that they were decreasing with Reynolds number.

4. Upstream effects where the boundary layer was laminar before separation, change rapidly with increasing Reynolds numbers, and are seen to be a function of the Reynolds number effect on the distance between separation and transition.

5. Pressure ratios required to cause separation in turbulent boundary layers, approximately 2.1, are almost double those required to cause separation in laminar boundary layers, approximately 1.1.

6. The pressure ratio at separation for both the laminar and turbulent boundary layers appear to be independent of shock strength and nearly independent of Reynolds number.

7. When the separated region is small, that is for small shock strength, the interaction phenomena is different than when the region is large. The pressure gradients appear to be larger when the separated region is small.

8. Shock wave types (impulse and step) should be distinguished and the results for a shock strength of one type should not be used with the results for a different shock strength of the other type in an interaction analysis.

REFERENCES

1. Ferri, Antonio: Experimental Results with Aerofoils Tested in the High-Speed Tunnel at Guidonia (1939). NACA TM 946, 1940.

2. Liepman, Hans W., Roshko, A., and Dhawan, S.: On Reflection of Shock Waves From Boundary Layers. NACA TN 2334, 1951.

3. Ackeret, J., Feldman, F., and Rott, N.: Investigations of Compression Shocks and Boundary Layers in Gases Moving at High Speed. NACA TM 1113, 1947.

4. Gadd, G. E., Holder, D.W., and Regan, J.D.: An Experimental Investigation of the Interaction Between Shock Waves and Boundary Layers. Proc. Roy. Soc. A. vol 226, p. 227 (1954).

5. Crocco, L. and Lees, L. : A Mixing Theory for the Interaction between Dissipative Flows and Nearly Isentropic Streams. J. Ae. Sc. vol. 19, No. 10, 1952.

6. Lighthill, M. J. : On Boundary Layers and Upstream Influence; Part II Supersonic Flows with Separation. Proc. Roy. Soc. A., vol. 217, p. 478, 1953.

7. Gadd, G. E.: Interactions Between Wholly Laminar and Wholly Turbulent Boundary Layers and Shock Waves Strong Enough to Cause Separation. J. Ae. Sc. vol. 20, No. 11, 1953.

8. Fage, A. and Sargent, R. F.: Shock Wave and Boundary Layer Phenomena Near a Flat Surface. Proc. Roy. Soc. A. vol. 190, p. 1, 1947.

9. Bogdonoff, S. M., Kepler, C. E., and Sanlorenzo, E.: A Study of Shock Wave Turbulent Boundary Layer Interaction at M. 3. Princeton Univ. Ae. Engr. Lab. Report No. 222, 1953.

10. Probestein, R. F., and Lin, C. C.: A Study of the Transition to Turbulence of the Laminar Boundary Layer at Supersonic Speeds. Inst. Ae. Sc. Preprint No. 596, 1956.

11. Bradfield, W. S., DeCoursin, D. G., and Blumer, C.B.: The Effects of Leading-Edge Bluntness On A Laminar Supersonic Boundary Layer. J. Ae. Sc. vol. 21, No. 6, 1954.

12. Dailey, C. L. and Wood, F. C.: Computational Curves for Compressible Fluid Problems. 1st edition, John L. Wiley & Sons Inc., 1949.

13. Oswatitsch, K. and Wieghardt, K. : Theoretical Analysis of Stationary Potential Flows and Boundary Layers at High Speed. NACA TM 1189 (translated). 1948.

14. Tsien, H. S. and Finston, M.: Interaction Between Parallel Streams of Subsonic and Supersonic Velocities. J. Ae. Sc. vol. 16, No. 9, 1949.

15. Stewartson, K. : On Interaction Between Shock Waves and Boundary Layers. Proc. Cambridge Phil. Soc. vol. 47, part 3, 1951.

16. Ritter, A. and Kuo Y. H. : Reflection of a Weak Shock from a Boundary Layer Along a Flat Plate. NACA TN 2868, 1953.

17. Holder, D. W.: The Interaction Between Shock Waves and Boundary Layers. Institute Ae. Sc. Preprint No. 550, 1955.

18. Moynihan, Fredrick: Normal Shock-Boundary Layer Interaction Studies on Cones at Mach Number 1.5. Univ. of Minnesota, Rosemount Aeronautical Lab. Research Report 136, 1956.

19. Holder, D. W., Pearcey, H. H. and Gadd, G. E.: The Interaction Between Shock Waves and Boundary Layers. British A,R.C. No. 16,526, C.P. No. 180, 1954.

20. Koepcke, W. W. : Interaction Between Laminar Boundary Layers and Shock Waves With Separation of Flow. Masters Thesis, University Of Minnesota, May 1957.

21. Schlichting, Herman: Boundary Layer Theory. McGraw - Hill Inc., New York, 1955.

22. Hermann, R. : Supersonic Inlet Diffusers and Introduction To Internal Aerodynamics. Minneapolis Honeywell Regulator Company, Minneapolis, Minnesota, 1956.

APPENDIX 1

EQUIPMENT DESIGN

General - The main problem encountered in the design of the equipment for this study was that of choking the test section. This problem was considered for four separate regions. These were:

1. Choking between the wedge and the upper wall.
2. Choking between the wedge and the flat plate.
3. Choking between the flat plate and the lower wall.
4. Choking from all of these obstructions in the test section.

All the calculations involving choking conditions and the subsequent design of the equipment were made with conservative assumptions. For example where boundary layer thickness was a criterea, the value based on turbulent Reynolds numbers was used and the boundary layer was assumed turbulent from the nozzle throat.

The calculations here were based on a stagnation chamber pressure of 100 p.s.i.a. at $59^{\circ}F$ for a Reynolds number per foot of 16.68×10^{6}, and on a stagnation chamber pressure of 14.7 p.s.i.a.

at 59° F for a Reynolds number per foot of 2.47×10^6 . Since the displacement thickness indicates the amount the free stream streamlines are shifted due to boundary layer formation, the displacement thickness was determined along the top and bottom tunnel walls and along the top and bottom of the wedges and of the flat plate. The turbulent displacement thickness was determined using the relation from Ref. 21:

$$\delta^* = \frac{\delta}{8} = \frac{1}{8} \left\{ \frac{0.37\, x_t}{(Re_{x_t})^{1/5}} \right\}$$

and the laminar displacement thickness was determined using the relation given in Ref. 7.

$$\delta^* = 1.721 \left[1 + 0.693(\gamma - 1) M_\infty^2 \right] \frac{x}{(Re_x)^{1/2}}$$

The displacement thicknesses for both the top and bottom tunnel walls was based on the length of the nozzle blocks from the throat position which, in this case, was 16 inches. The additional length of the upper wall due to the nozzle contour was neglected. The plate and wedges were assumed to

be 4.5 inches long. These values were then computed to be

	Turbulent	Laminar
δ^*	walls - 0.025 inches	0.0790 inches
δ^*	plates - 0.0087 inches	0.0284 inches

The flat plate thickness was 0.125 inches and the wedge thicknesses were 0.125 inches and 0.25 inches. The choice of these values will be discussed later under the design of each component. The wedge and flat plate mounting pylon thicknesses were 0.125 inches. Using these dimensions and the swallowing function, ϑ, for the free stream Mach number 3.03, $\vartheta = 0.718$ from Ref. 22, the previously stated choking conditions were investigated and the required clearances found are summarized in the table below. The relation used in determining the required clearances was also from Ref. 22, and is

$$\frac{A_2}{A_1} = \vartheta(M)$$

where A_1 is the capture area, and

A_2 is the swallowing area.

TABLE I

Regions	Boundary Layer State	.25 in. wedge	.125 in. wedge
1	Laminar Turbulent	*No Choking Wedge pylon height determined by boundary layer thickness .20 inches.	
**	Laminar	0.840 in.	.521 in.
2	Turbulent	0.695 in.	.380 in.
3	Laminar	0.785 in.	.785 in.
	Turbulent	0.563 in.	.563 in.
4	Laminar	0.9637 in.	.815 in.
	Turbulent	0.964 in.	.815 in.

* No choking occurs between the upper tunnel wall and the wedge because of the nozzle block curvature. That is this channel behaves somewhat like a diffuser section in that it is opening faster than the displacement thickness and the pylon thickness act to reduce the area.

** Most critical configuration existed when the leading edges of the wedge and plate were even.

Since all of the channel heights determined above for the critical boundary layer condition, laminar ($\frac{1}{4}$" wedge) sum to a greater height than the test section height of 1.94 inches, some compromises were made. The minimum channel height between the wedge and the flat plate excluding boundary layer build up was calculated to be 0.638 inches. This value made a flat plate height of 0.727 possible which was above the value computed for the turbulent boundary layer. Therefore, it was decided to split the difference here and make the flat plate pylon height 0.715 and the height between the $\frac{1}{4}$ inch wedge and the flat plate was increased to 0.650 inches.

The final channel heights computed here were 0.20 inches between upper wall and wedge, 0.650 inches between the $\frac{1}{4}$ inch wedge and the flat plate and 0.715 inches between the flat plate and the lower wall.

Flat Plate - In order to alleviate any three dimensional effects on the results of this investigation the flat plate was made to span the tunnel. From previous work in this tunnel a plate

thickness of 0.125 inches was the minimum thickness considered compatible with the rigidity required. The physical dimensions of the plate then were 1.75 inches wide by 4.50 inches long and 0.125 inches thick. This length was chosen to permit an unobstructed area for the static pressure taps ahead of the mounting pylon, see Fig. 2. The leading edge was made as sharp as possible by a 5° wedge angle on the underneath side.

Since this investigation was to be based on a static pressure survey along the surface of the flat plate, the question of pressure tap size and spacing arises. As given in Ref. 18, for turbulent flow, the pressure tap diameter should be no greater than 15 per cent of the apparent shock thickness which was given by the relation

$$t - h = \frac{C\, a\, x_t}{Re_{x_t}^{1/n}}$$

Since the shock thickness was found to be considerably smaller for turbulent boundary layers than for laminar, Ref. 2, evaluation of the above relation was made where for turbulent flow

$$n = 5$$

$$a = 10$$

$$C = .365$$

x = distance from the effective leading edge of the turbulent boundary layer, estimated from the transition position.

Based on a Reynolds number per foot of 16.68×10^6 and a value of x_t to the first pressure tap of 0.25 inches, the apparent shock thickness was determined to be 0.071 inches. In this case a maximum tap diameter should be no greater than 0.0106 inches. A tap diameter of 0.006 inches was chosen to further reduce the effect of hole size on the measured shock thickness.

The longitudinal spacing of the pressure taps was chosen to obtain an equitable Reynolds number variation in addition to any variation obtained by changing the stagnation pressure. In this case, as shown in Fig. 2, five holes were equally spaced at 0.25 inches on centers. The first hole was placed 0.725 inches aft of the flat plate leading edge to eliminate or reduce leading edge effects as much as possible. Such effects as leading edge thickness and vibration tend to reduce the transition Reynolds number as given by Ref. 10. The holes were staggered, as shown in Fig. 2, to reduce the interference effects between taps as much as possible.

The last hole was placed on the center line one inch aft of the first hole well within the Mach wave boundaries off the leading edge corners of the plate. At Mach number 3 the wave angle was 19.3° and as seen in the figure all holes were placed with an area bounded by an equivalent wave angle of 23° for additional safety.

Shock Generators - The shock generators were half wedges which were movable relative to the fixed flat plate. Since it was desired to vary the shock strengths in this investigation, various wedge angles were chosen from 5° to the maximum possible, 15° in this case. For the test section Mach number 3.03 the maximum wedge angle capable of producing an attach shock was 33.2°.

The maximum wedge angle was limited to 15° by two factors, namely (1) the interference of the expansion from the back of the wedge with the incident shock wave, and (2) the wedge thickness was limited by the choking conditions in the test section. For example; the minimum distance between a 0.3125 inch thick wedge and the flat plate was computed to be 0.92 inches which would then not

permit the clearances required between the flat plate and the lower wall and the wedges and the upper wall. Hence the thickest wedge feasible to use was 0.25 inches thick. From Fig. 15, it is seen that for a 15° wedge angle and minimum separation between wedge and flat plate the separation between the incident shock and the expansion fan is 0.259 inches. Since this is only slightly greater than the anticipated turbulent interaction length, any appreciably larger wedge angle would result in an interference of the incident shock by the expansion on the back of the wedge.

It was interesting to note how closely the above calculated conditions were to the actual conditions found in the tunnel. As will be observed, the data for the 0.25 inch 15° wedge is incomplete. This resulted from the extreme difficulty experienced in starting the tunnel with this configuration. On some occassions it was impossible to start the tunnel regardless of the conditions of the test, i.e. vacum and stagnation pressures used, because of the choking conditions existing in the test section. After 0.050 inches was removed from the wedge pylon, or a tunnel obstruction area reduction of .00625 sq. inches, the tunnel operated satisfactorily.

A check of the quipment installed in the tunnel revealed the following changes that resulted from fabrication tolerances:

1. the 0.25 inch wedge was actually 0.240 inches
2. the 0.125 inch flat plate was 0.120 inches
3. the flat plate pylon height was 0.715 in. fwd.
   0.712 in. aft.

The channel between the 0.25 inch wedge and the flat plate was 0.620 inches measured at the back of the wedge and 0.765 inches measured at the ends of the wedge plate and the flat plate. The increase at the end of the plate is due in part to the .125 inch step located one inch aft of the back of the wedge, visible in Fig. 16. The remaining 0.030 inches is attributed to the inaccuracies in the tunnel set up and in the fabrication of the equipment. If these values are used and the boundary layer effects are neglected we see

$$\frac{A_2}{A_1} = \frac{0.620}{0.860} = 0.721 > 0.718$$

$$A_1 = 0.620 + 0.240$$

which indicates the internal channel, region 2, was within 0.42 per cent of the swallowing function given in Ref. 22.

Lead Screw Mechanism - Because of the previously mentioned problems of choking in the test section it became evident early in the study that some external means of accurately positioning the wedges would be required. This was accomplished by means of a lead screw in the following manner. A section of the upper plastic nozzle block five inches long was cut out parallel to the bottom test section wall. This cut was made in an area where the nozzle block was a straight tapering section. The removed section was then replaced in the cut section a "T" slot which carried the wedge mounting pylon, resulted. A lead screw operating through a brass plug in the flange between the tunnel test section and the diffuser section was attached to the wedge pylon in such a manner the pylon could be moved fore and aft in the slot by turning the lead screw. The pylon could be removed by removing one of the two blocks from the cut section which were held in place by machine screws.

The length of the slot determined in part by the length of the straight portion of the nozzle

block was also determined by the movement required of the wedges. That is the most forward position of the 5° wedge was the controlling factor on the most forward position of the wedge pylon in that the incident shock should be forward of the first tap. Similarly the most aft pylon position was determined by the incident shock from the 15° wedge such that it should be an interaction length aft of tap 5. In this manner the slot length required was found to be five inches.

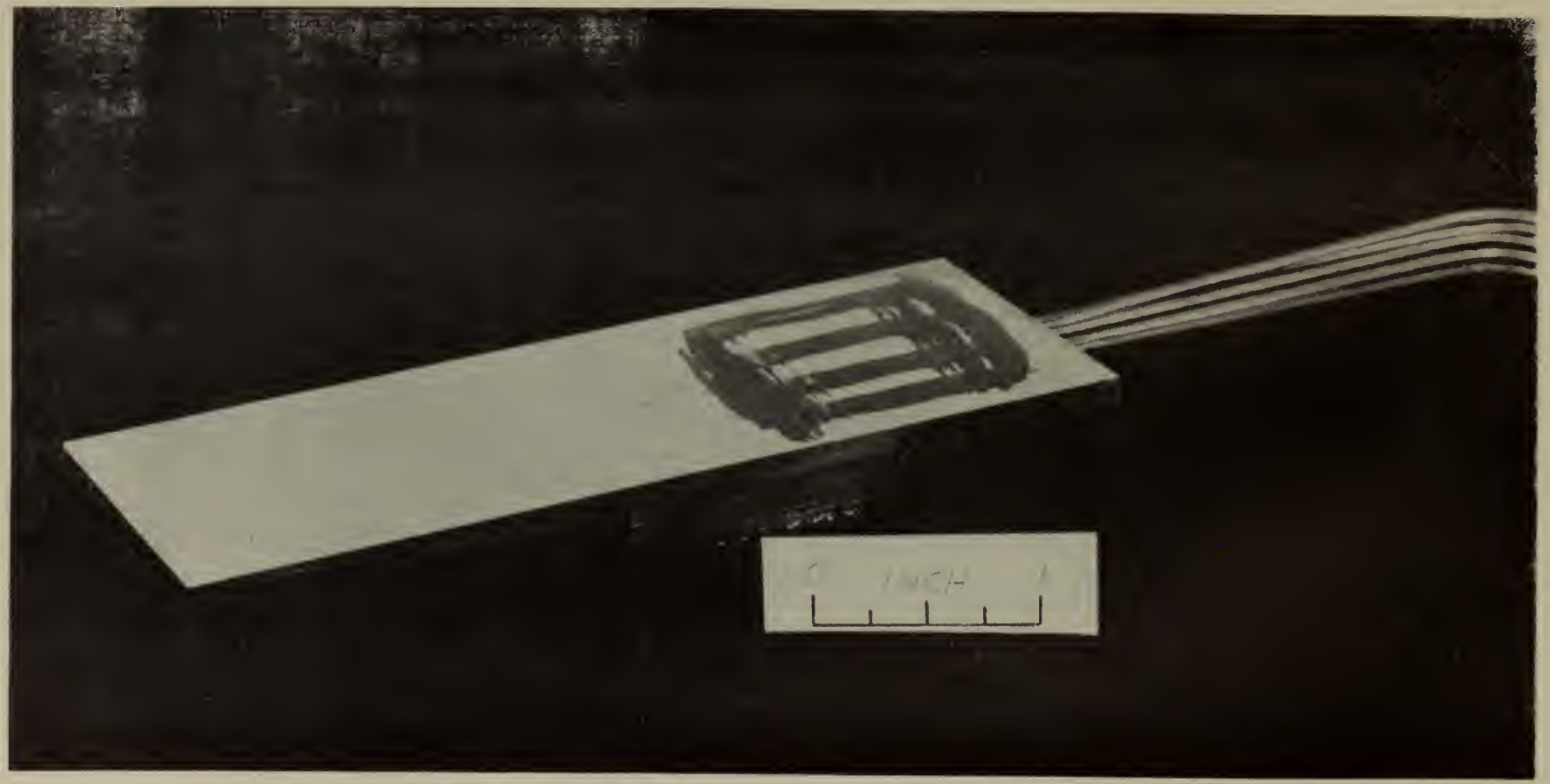

Fig. 1 (a)

FLAT PLATE

FIG. 1 (b)

5, 10, 15 DEGREE WEDGES

LEADING EDGE POINTS TO LEFT

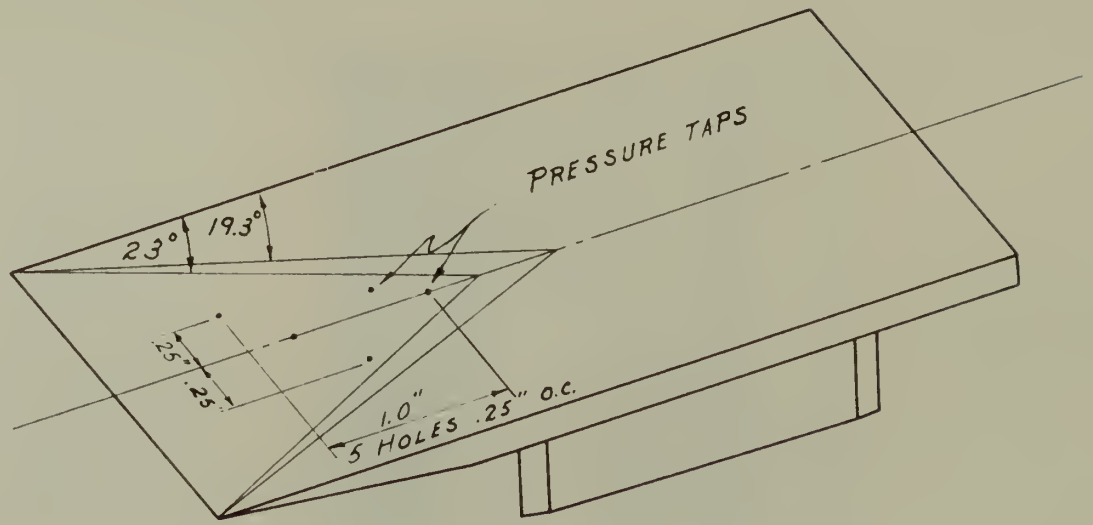

THE TAPS ARE NUMBERED CONSECUTIVELY AFT FROM THE LEADING EDGE.

FLAT PLATE LAYOUT

FIG. 2

WIND TUNNEL SHOWING

THE ASYMMETRIC NOZZLE

FIG. 3

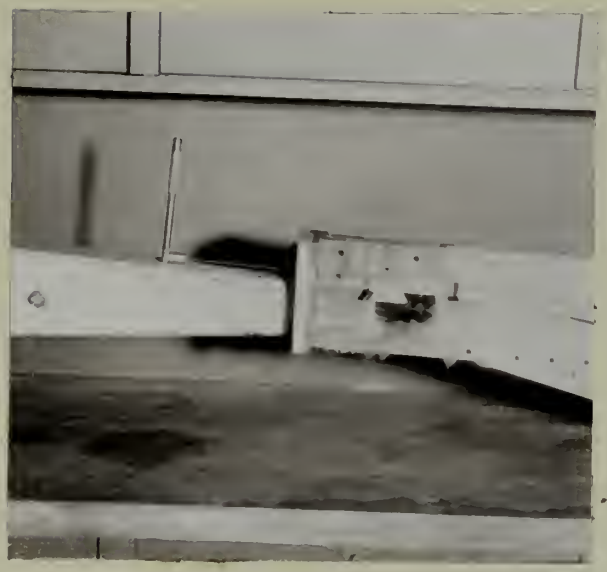

WEDGE PYLON AND LEAD SCREW

MECHANISM

FIG. 4

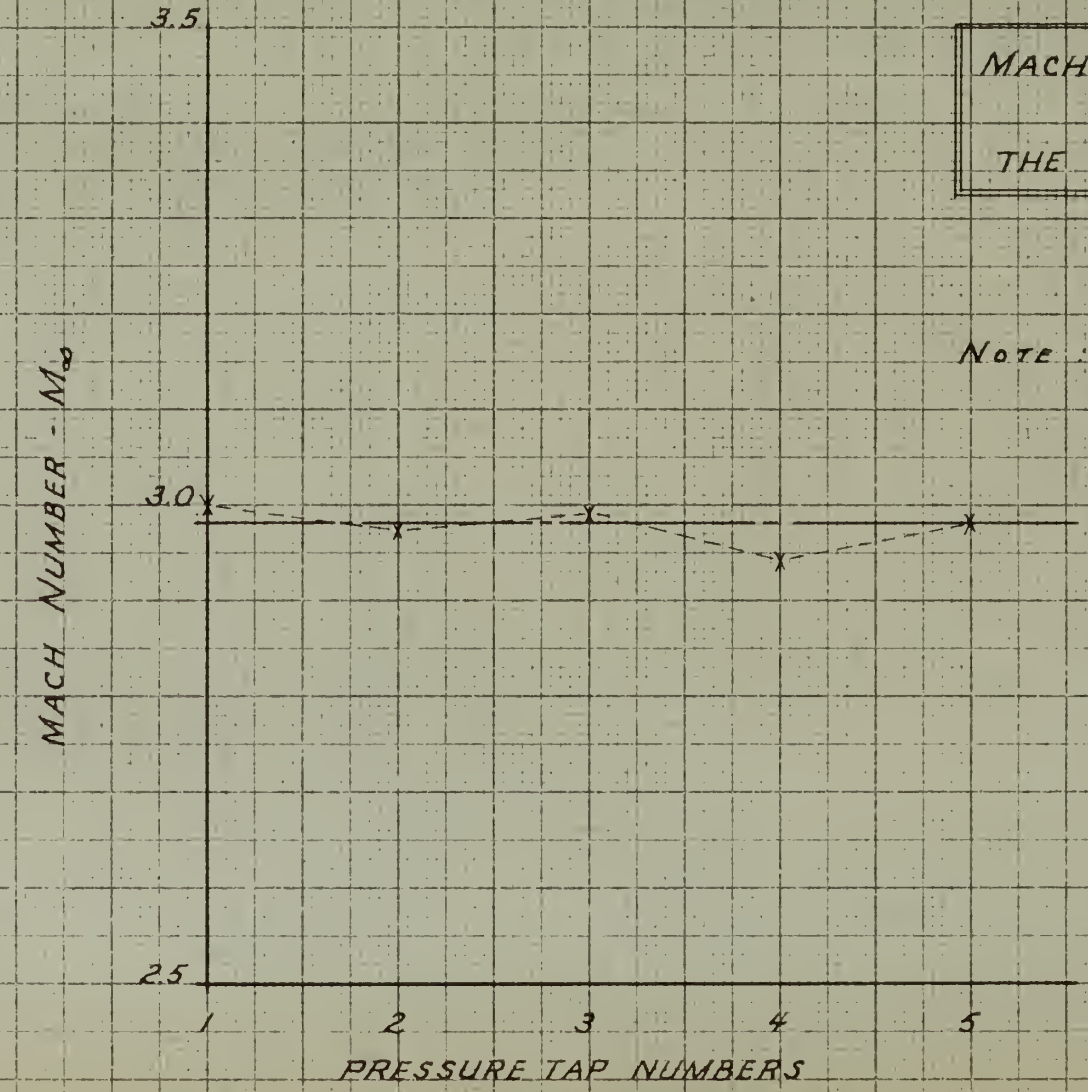

MACH DISTRIBUTION
OVER
THE FLAT PLATE

NOTE : TAP POSITIONS AS
GIVEN IN FIG. 2.

FIG. 5

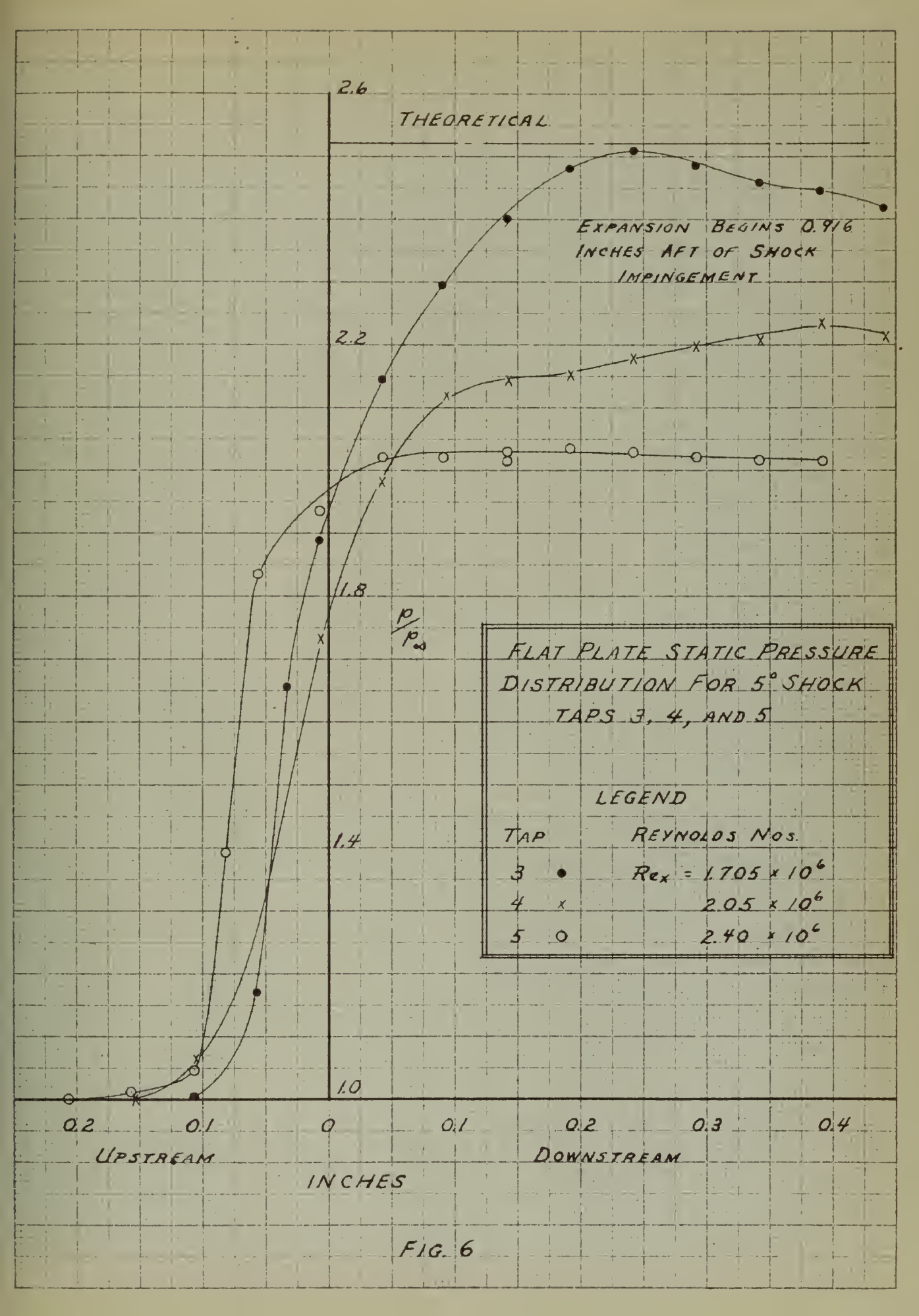
2.6
THEORETICAL
EXPANSION BEGINS 0.916 INCHES AFT OF SHOCK IMPINGEMENT
2.2
1.8
p/p∞
1.4
1.0
FLAT PLATE STATIC PRESSURE DISTRIBUTION FOR 5° SHOCK TAPS 3, 4, AND 5
LEGEND
TAP
REYNOLDS Nos.
3 • Rex = 1.705 × 10^6
4 x 2.05 × 10^6
5 o 2.40 × 10^6
0.2
0.1
0
0.1
0.2
0.3
0.4
UPSTREAM
DOWNSTREAM
INCHES

FIG. 6

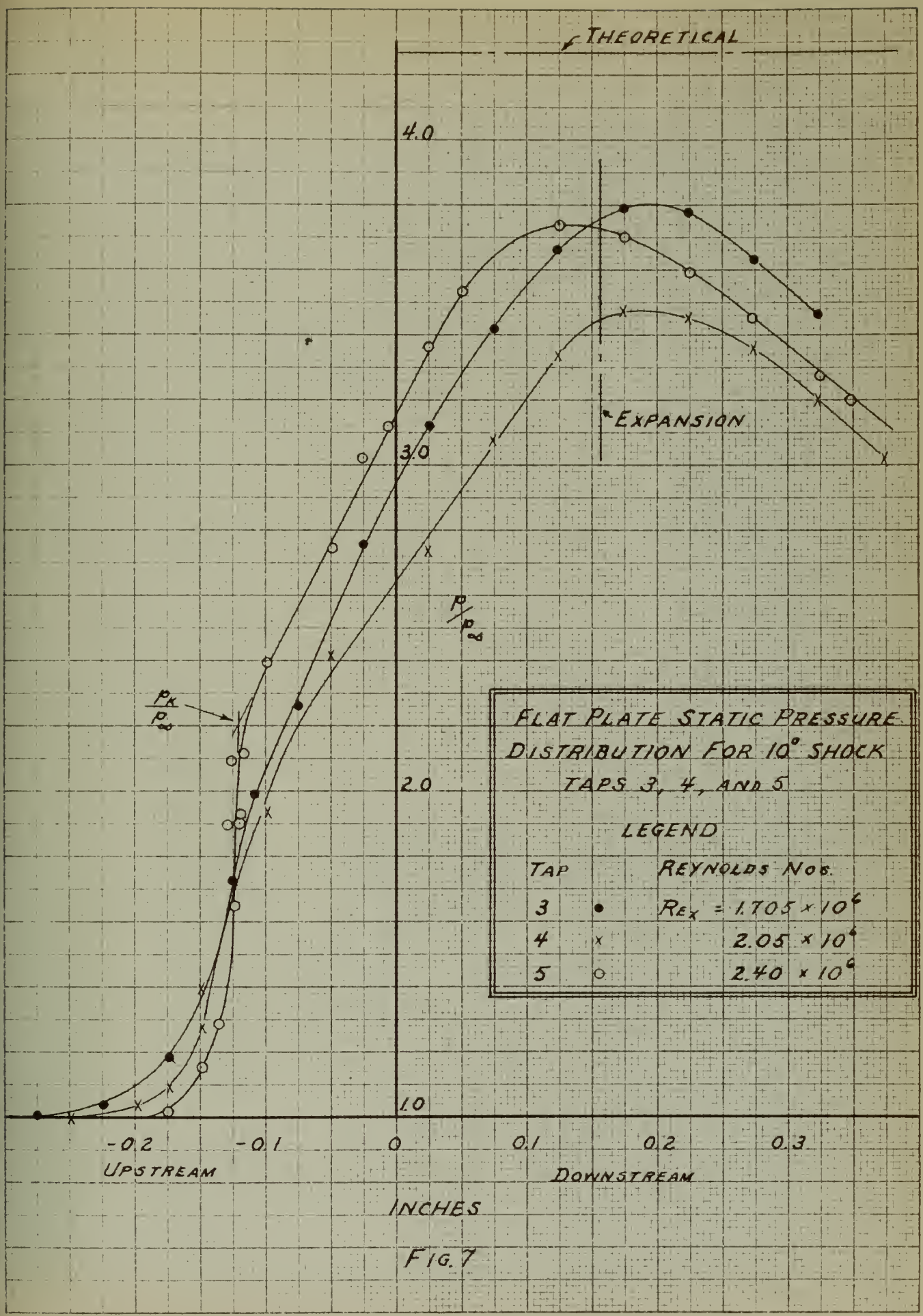
THEORETICAL
4.0
3.0
2.0
1.0
EXPANSION
$\frac{p}{p_\infty}$
$\frac{p_x}{p_\infty}$
FLAT PLATE STATIC PRESSURE DISTRIBUTION FOR 10° SHOCK
TAPS 3, 4, AND 5
LEGEND
TAP
REYNOLDS NOS.
3 • $R_{e_x} = 1.705 \times 10^6$
4 x 2.05 x 10^6
5 ○ 2.40 x 10^6
-0.2
-0.1
0
0.1
0.2
0.3
UPSTREAM
DOWNSTREAM
INCHES

FIG. 7

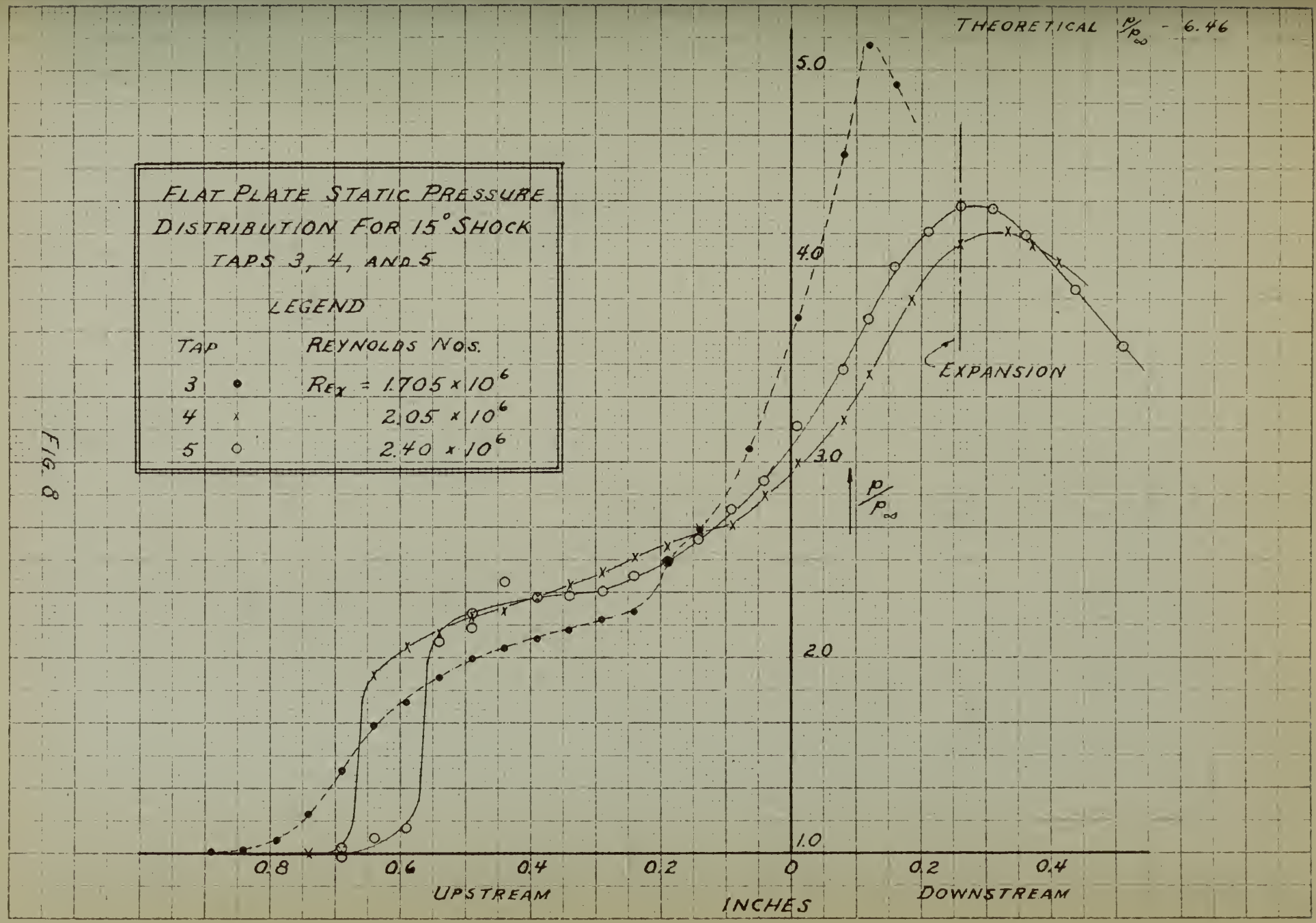
FLAT PLATE STATIC PRESSURE DISTRIBUTION FOR 15° SHOCK
TAPS 3, 4, AND 5
LEGEND
TAP
REYNOLDS NOS.
3 • R_{e_x} = 1.705 × 10^6
4 × 2.05 × 10^6
5 ○ 2.40 × 10^6
THEORETICAL p/p_∞ = 6.46
5.0
4.0
3.0
2.0
1.0
p/p_∞
EXPANSION
0.8
0.6
0.4
0.2
0
0.2
0.4
UPSTREAM
INCHES
DOWNSTREAM
FIG 8

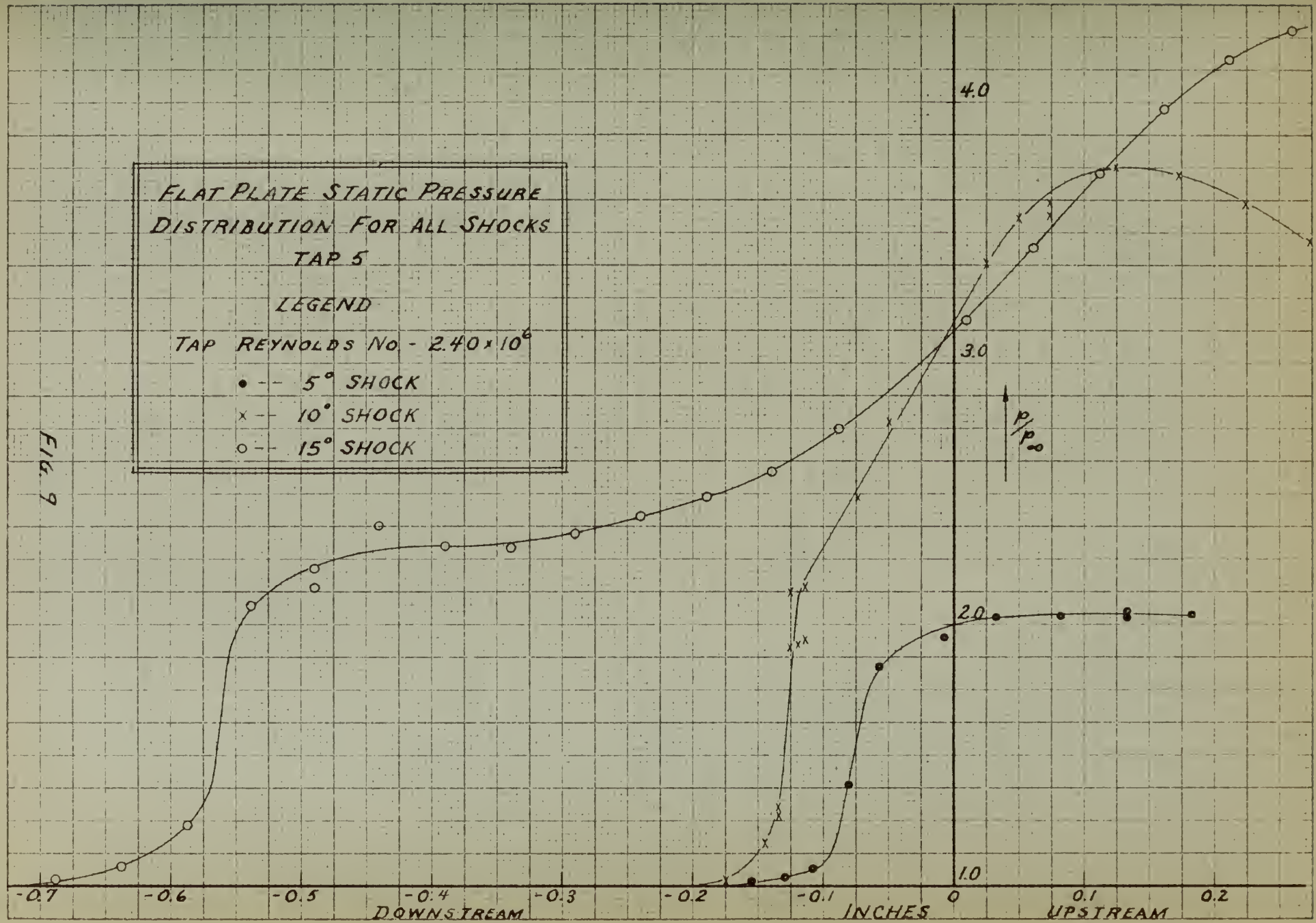
FLAT PLATE STATIC PRESSURE
DISTRIBUTION FOR ALL SHOCKS
TAP 5
LEGEND
TAP REYNOLDS NO. - 2.40 x 10^6
• -- 5° SHOCK
x -- 10° SHOCK
o -- 15° SHOCK
FIG. 9
4.0
3.0
2.0
1.0
p/p∞
-0.7
-0.6
-0.5
-0.4
-0.3
-0.2
-0.1
0
0.1
0.2
DOWNSTREAM
INCHES
UPSTREAM

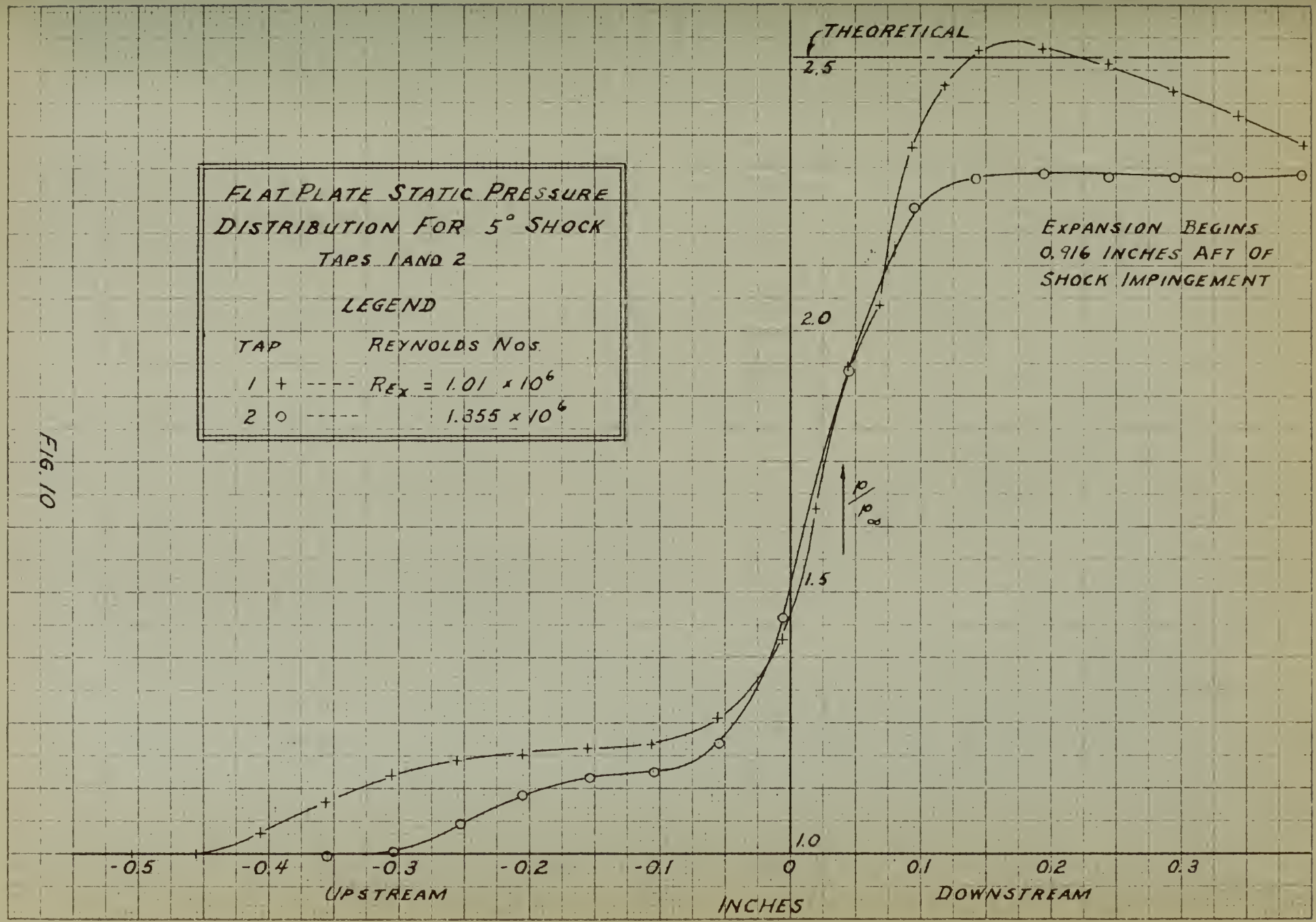
FLAT PLATE STATIC PRESSURE DISTRIBUTION FOR 5° SHOCK
TAPS 1 AND 2
LEGEND
TAP REYNOLDS NOS.
1 + ---- R_{E_x} = 1.01 x 10^6
2 ○ ----- 1.355 x 10^6
THEORETICAL
2.5
2.0
1.5
1.0
p/p_∞
EXPANSION BEGINS
0.916 INCHES AFT OF
SHOCK IMPINGEMENT
-0.5
-0.4
-0.3
-0.2
-0.1
0
0.1
0.2
0.3
UPSTREAM
INCHES
DOWNSTREAM

FIG. 10

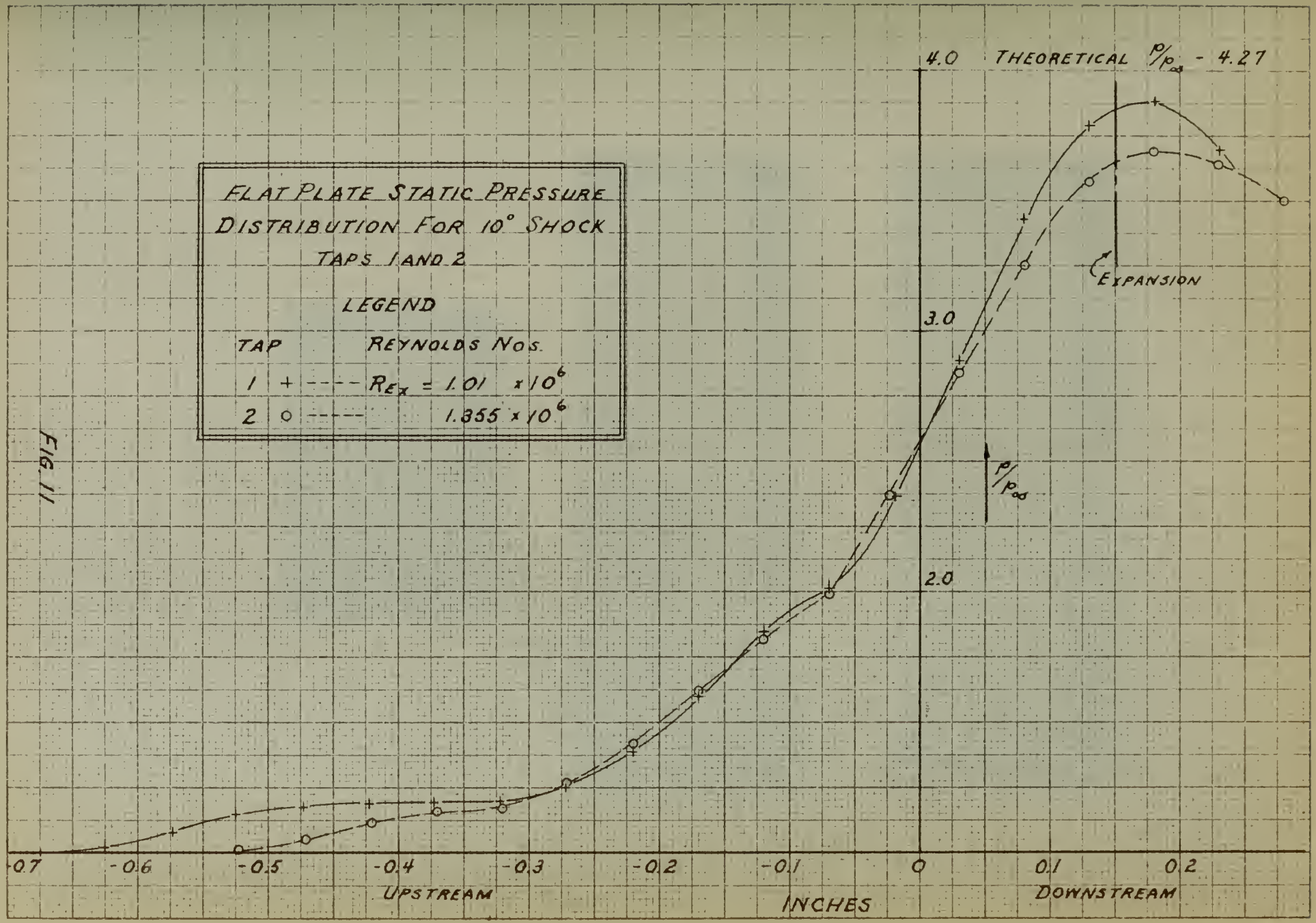
FLAT PLATE STATIC PRESSURE DISTRIBUTION FOR 10° SHOCK
TAPS 1 AND 2
LEGEND
TAP REYNOLDS NOS.
1 + ---- R_{E_x} = 1.01 x 10^6
2 o ---- 1.355 x 10^6
4.0 THEORETICAL p/p_∞ - 4.27
EXPANSION
3.0
2.0
p/p_∞
-0.7 -0.6 -0.5 -0.4 -0.3 -0.2 -0.1 0 0.1 0.2
UPSTREAM
INCHES
DOWNSTREAM

FIG 11

(1)
Re_x - 1.01 x 10^6

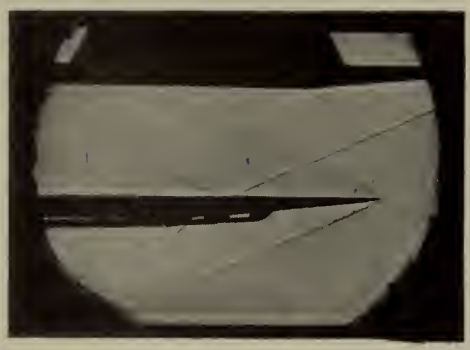

(2)
Re_x - 1.355 x 10^6

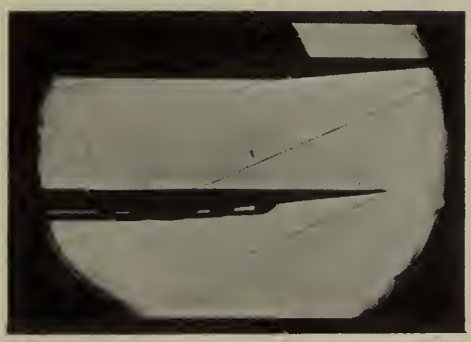

(3)
Re_x - 1.705 x 10^6

(4)
Re_x - 2.05 x 10^6

(5)
Re_x - 2.40 x 10^6

SHADOWGRAPHS - 5° SHOCK

Fig. 12 (a)

(1)
Re_x-1.01 x 10^6

(2)
Re_x-1.355 x10^6

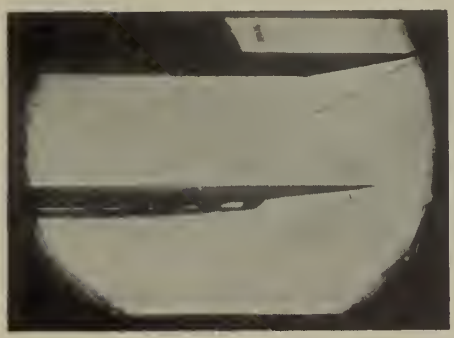

(3)
Re_x - 1.705 x 10^6

(4)
Re_x- 2.05 x 10^6

(5)
Re_x-2.40 x10^6

SHADOWGRAPHS - 10° SHOCK

Fig. 12 (b)

(4)

Re_x - 2.05×10^6

(5)

Re_x - 2.40×10^6

SHADOWGRAPHS - 15° SHOCK

Fig. 12 (c)

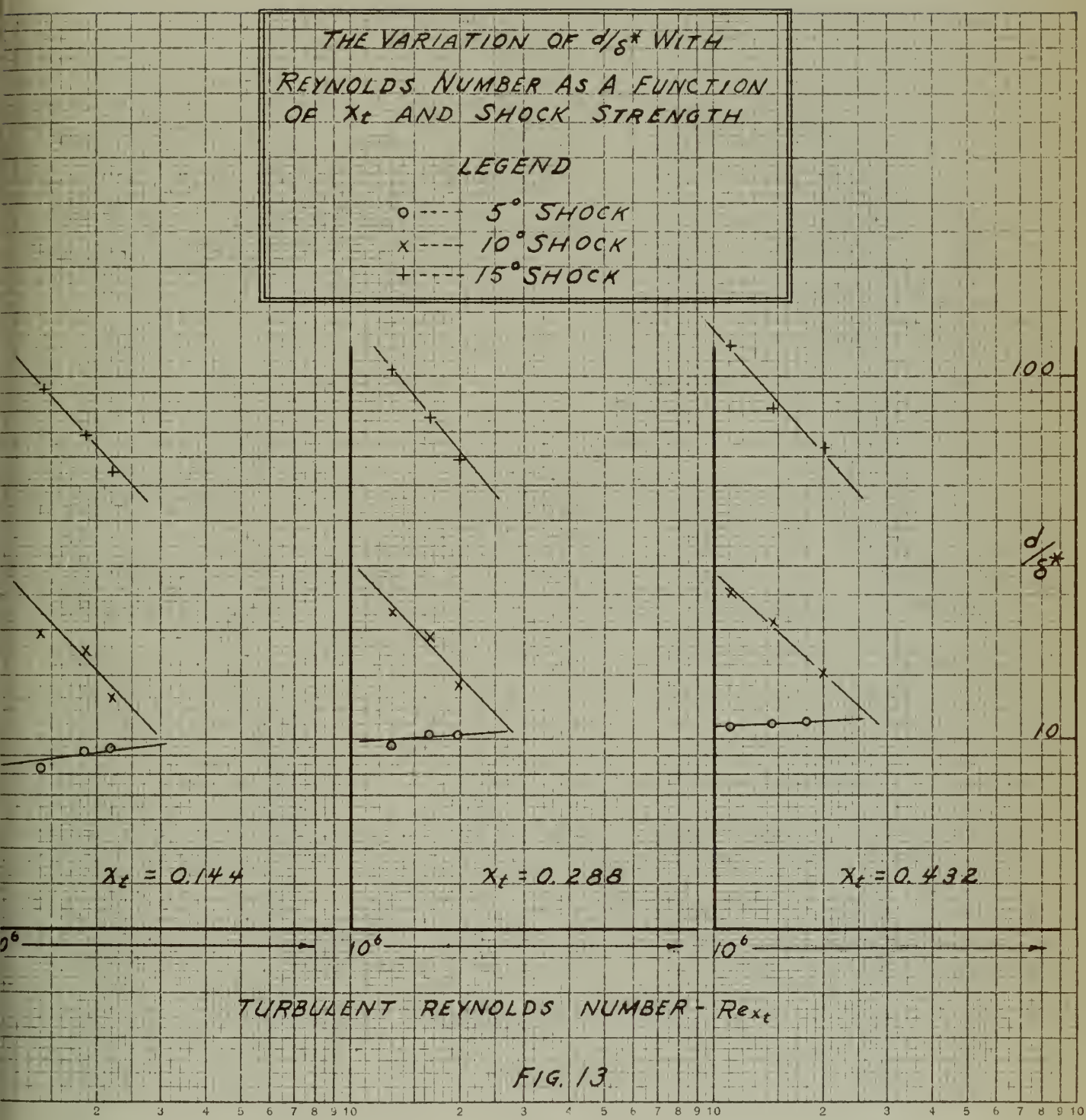
THE VARIATION OF d/δ* WITH
REYNOLDS NUMBER AS A FUNCTION
OF x_t AND SHOCK STRENGTH
LEGEND
o ---- 5° SHOCK
x ---- 10° SHOCK
+ ---- 15° SHOCK
100
d/δ*
10
x_t = 0.144
x_t = 0.288
x_t = 0.432
10^6
10^6
10^6
TURBULENT REYNOLDS NUMBER - Re_{x_t}
2 3 4 5 6 7 8 9 10
2 3 4 5 6 7 8 9 10
2 3 4 5 6 7 8 9 10

FIG. 13

FIG. 14

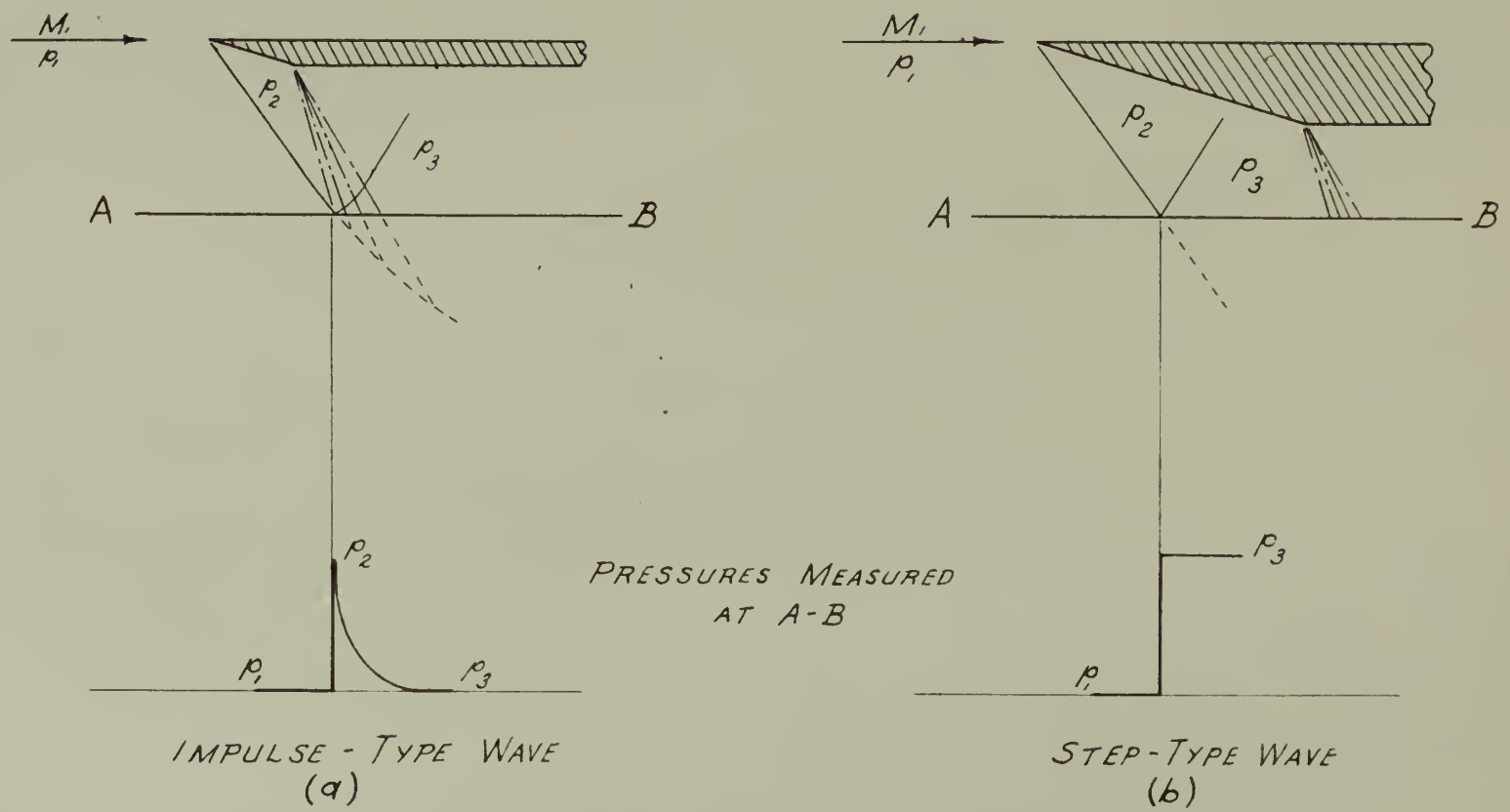

IMPULSE - TYPE WAVE
(a)

STEP - TYPE WAVE
(b)

IDEAL SHOCK WAVE TYPES

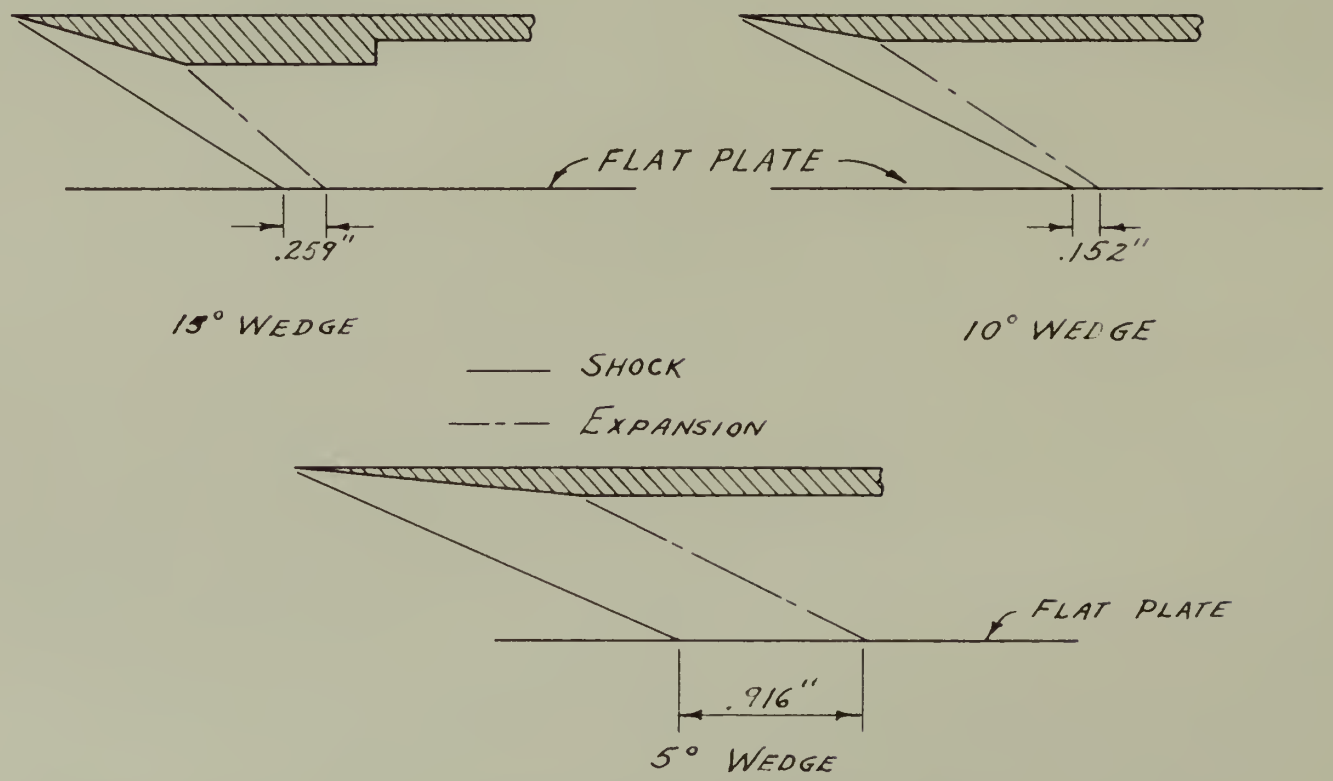

FIG. 15

SHOCK WAVE - EXPANSION FAN SEPARATIONS

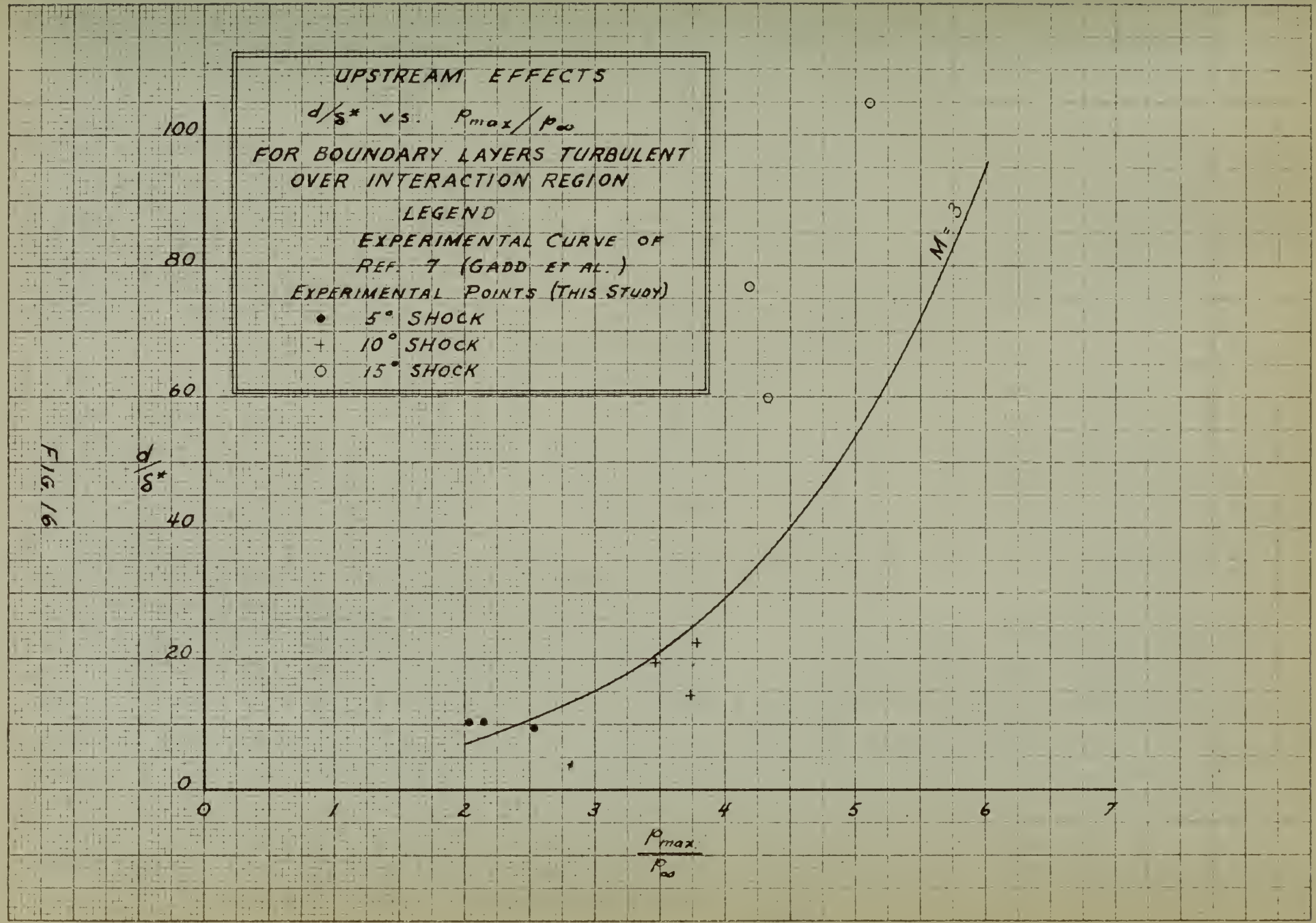
UPSTREAM EFFECTS
d/δ* vs. Pmax/P∞
FOR BOUNDARY LAYERS TURBULENT OVER INTERACTION REGION
LEGEND
EXPERIMENTAL CURVE OF REF. 7 (GADD ET AL.)
EXPERIMENTAL POINTS (THIS STUDY)
• 5° SHOCK
+ 10° SHOCK
○ 15° SHOCK
M=3
100
80
60
40
20
0
d/δ*
0
1
2
3
4
5
6
7
Pmax./P∞

FIG. 16

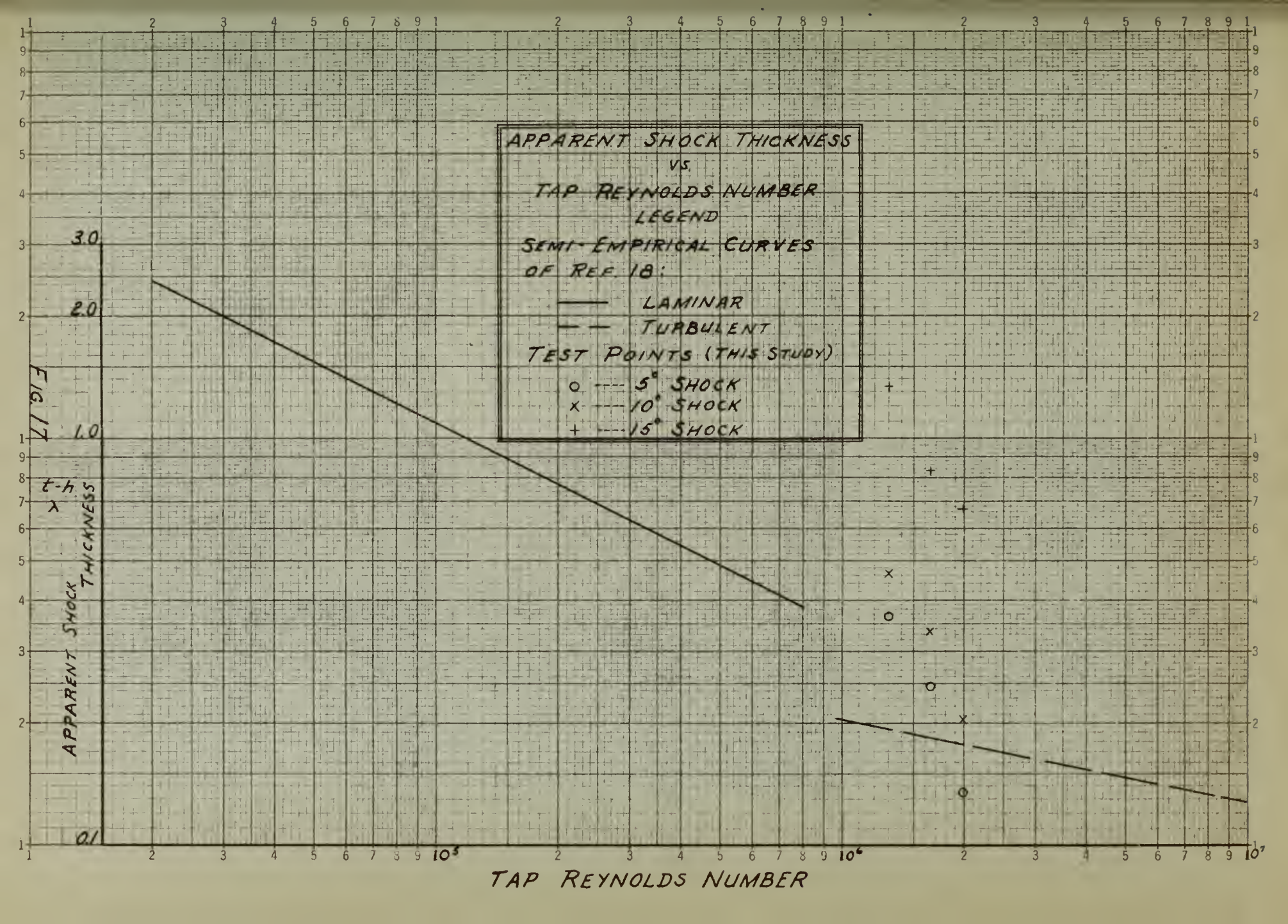
APPARENT SHOCK THICKNESS
VS.
TAP REYNOLDS NUMBER
LEGEND
SEMI-EMPIRICAL CURVES
OF REF. 18:
LAMINAR
TURBULENT
TEST POINTS (THIS STUDY)
5° SHOCK
10° SHOCK
15° SHOCK
FIG. 17
APPARENT SHOCK THICKNESS
$\frac{t-h}{\lambda}$
3.0
2.0
1.0
0.1
10^5
10^6
10^7
TAP REYNOLDS NUMBER

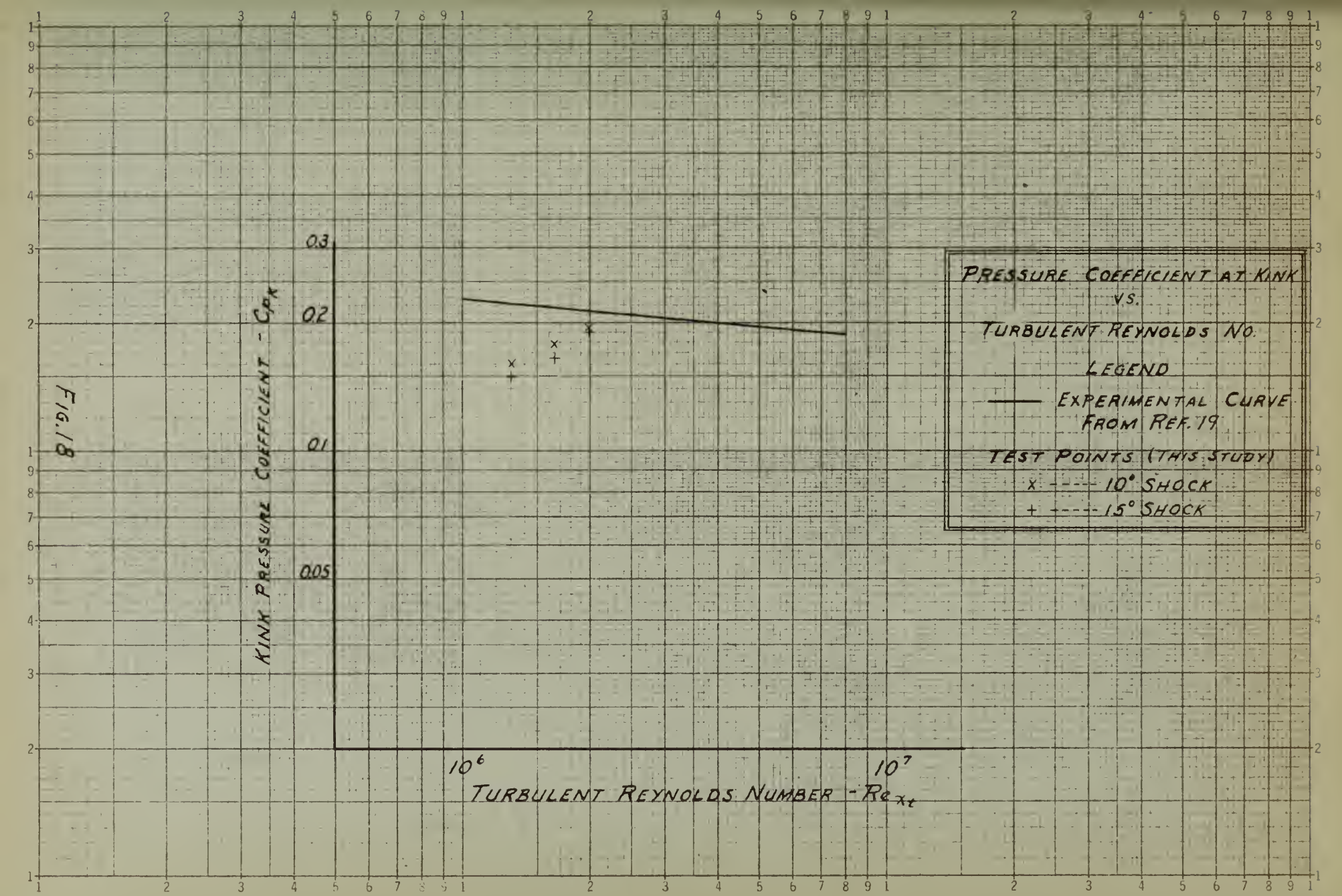
FIG. 18
KINK PRESSURE COEFFICIENT - C_{p_K}
0.3
0.2
0.1
0.05
10^6
10^7
TURBULENT REYNOLDS NUMBER - Re_{x_t}
PRESSURE COEFFICIENT AT KINK
VS.
TURBULENT REYNOLDS NO.
LEGEND
EXPERIMENTAL CURVE FROM REF. 19
TEST POINTS (THIS STUDY)
x ---- 10° SHOCK
+ ---- 15° SHOCK

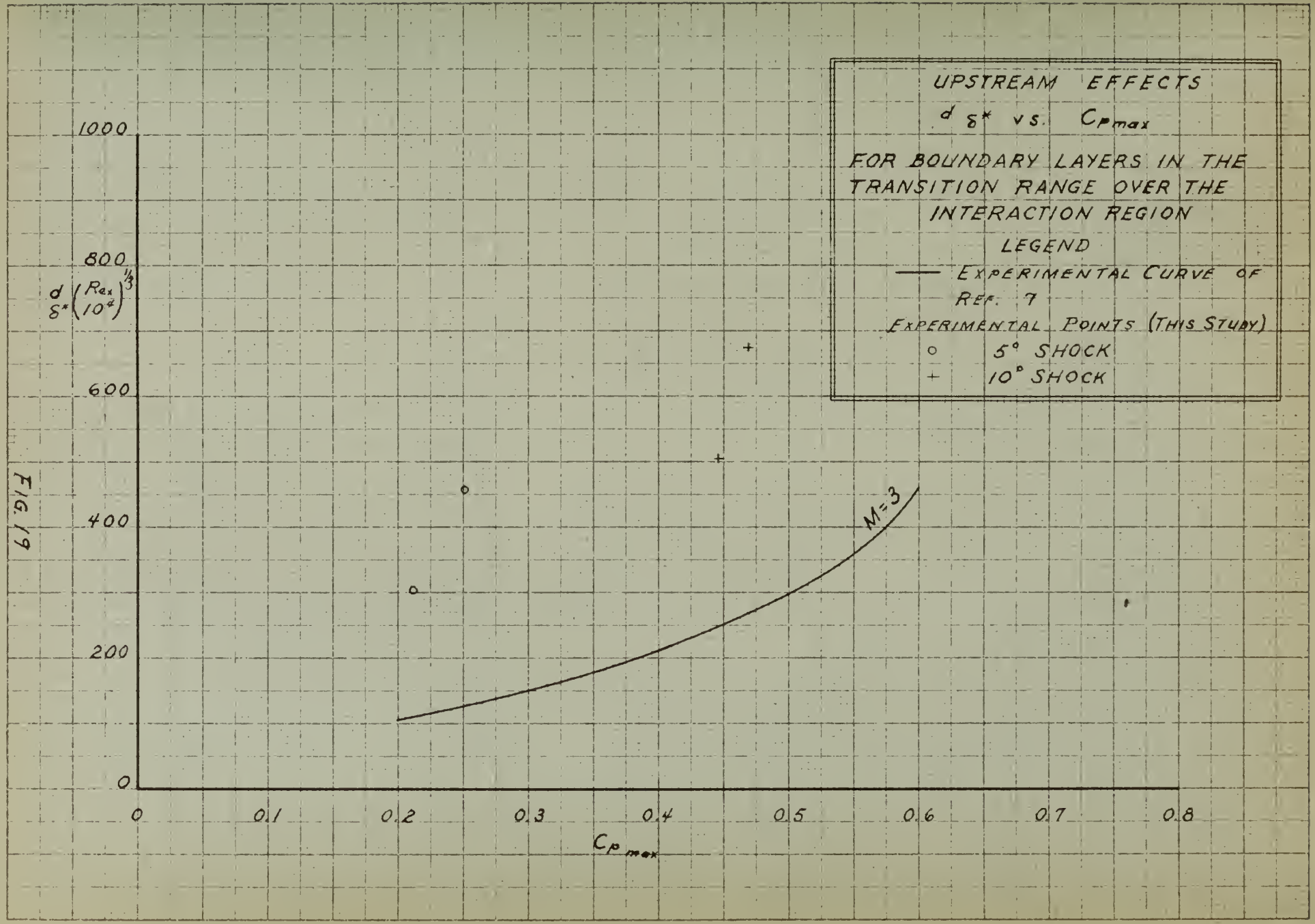
UPSTREAM EFFECTS
d δ* vs. Cp max
FOR BOUNDARY LAYERS IN THE TRANSITION RANGE OVER THE INTERACTION REGION
LEGEND
EXPERIMENTAL CURVE OF REF. 7
EXPERIMENTAL POINTS (THIS STUDY)
5° SHOCK
10° SHOCK
M=3
1000
800
600
400
200
0
d δ* (Rex / 10⁴)^1/3
0
0.1
0.2
0.3
0.4
0.5
0.6
0.7
0.8
Cp max
FIG 19

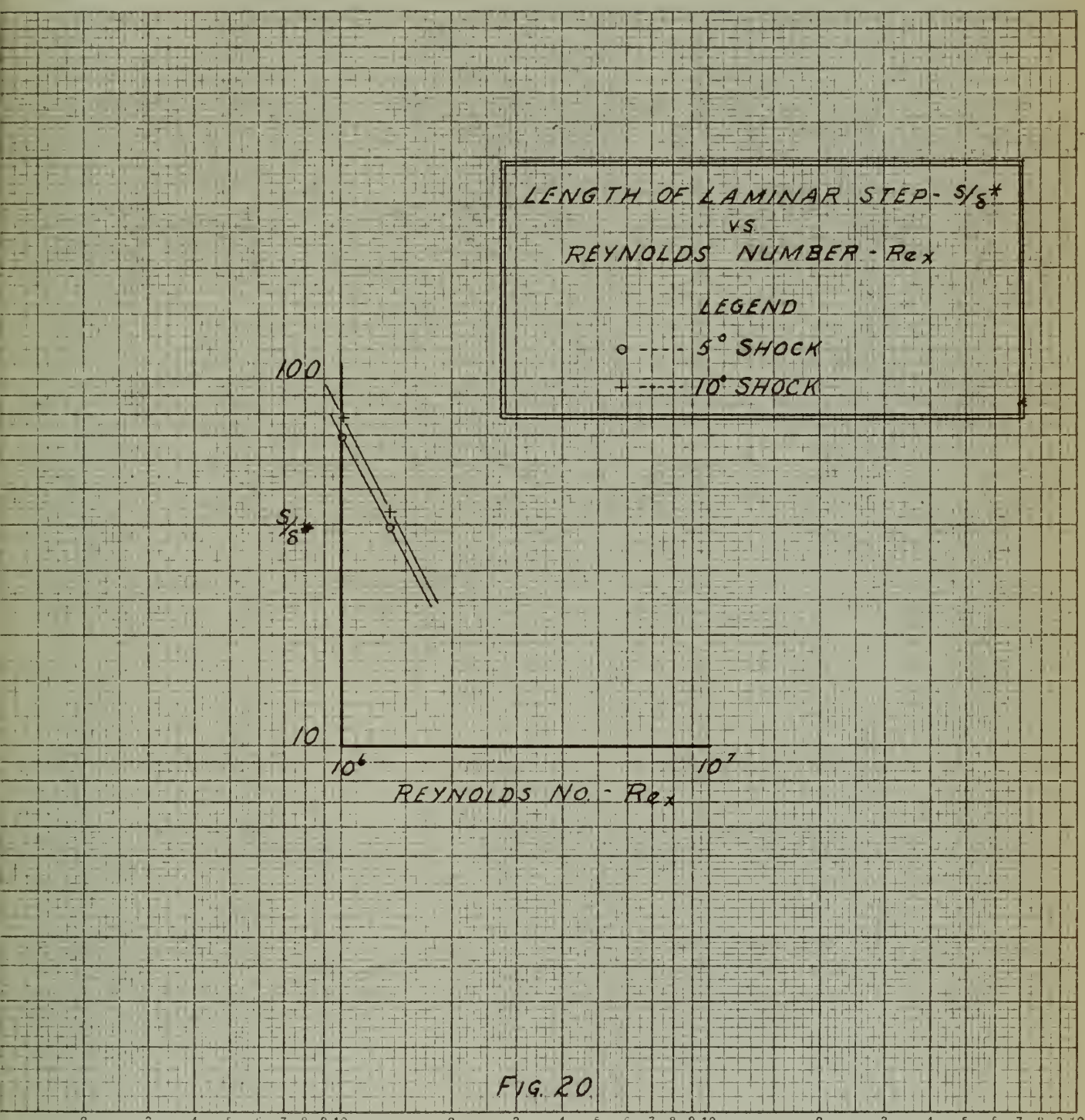
LENGTH OF LAMINAR STEP - δ/δ^*
VS.
REYNOLDS NUMBER - Re_x
LEGEND
o ---- 5° SHOCK
+ ---- 10° SHOCK
100
δ/δ^*
10
10^6
10^7
REYNOLDS NO. - Re_x
2 3 4 5 6 7 8 9 10
2 3 4 5 6 7 8 9 10
2 3 4 5 6 7 8 9 10

FIG. 20

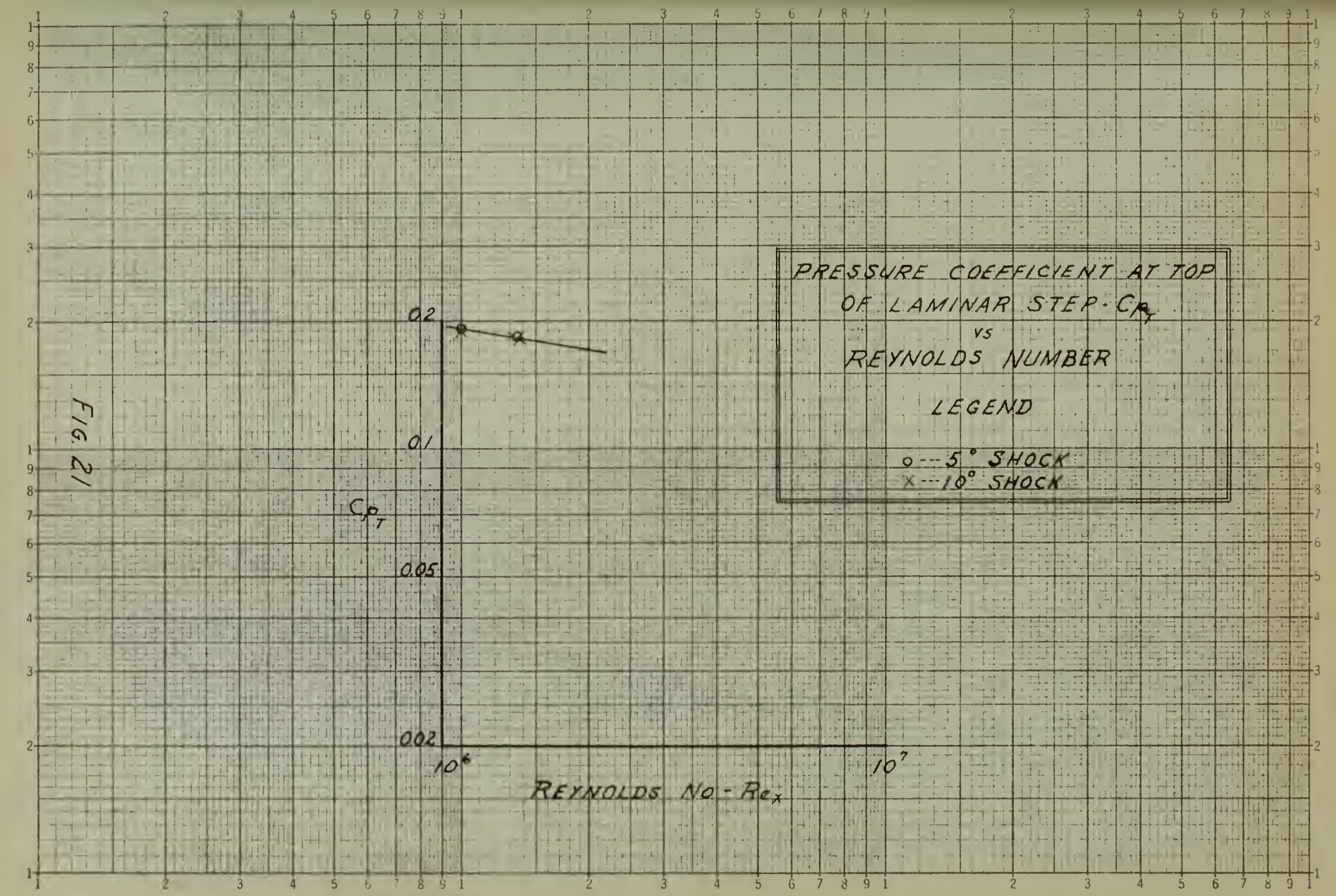
PRESSURE COEFFICIENT AT TOP OF LAMINAR STEP - C_{p_T}
VS
REYNOLDS NUMBER
LEGEND
o --- 5° SHOCK
x --- 10° SHOCK
0.2
0.1
0.05
0.02
C_{p_T}
10^6
10^7
REYNOLDS NO. - Re_x

FIG. 21

Thesis
I59
c.1

35886

Irish
Interaction between shock waves and turbulent or transitional boundary layers at mach number 3.